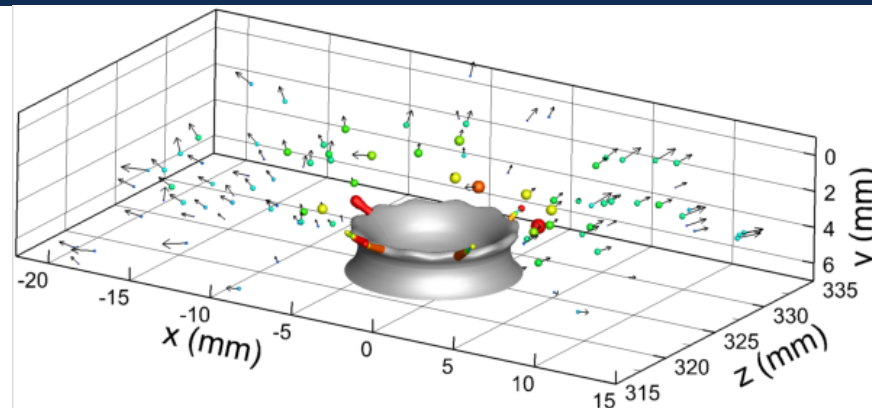
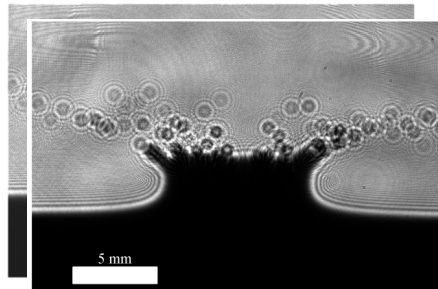


Exceptional service in the national interest



Digital In-line Holography (DIH) for 3D Quantification of Inert and Reacting Particle Fields

Daniel R. Guildenbecher

July 29, 2016

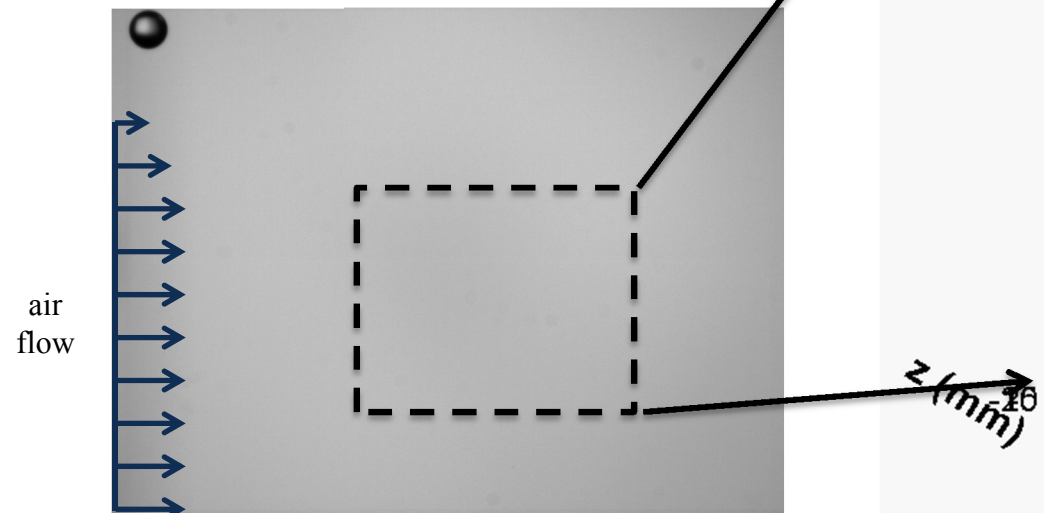


Sandia National Laboratories is a multi-program laboratory managed and operated by Sandia Corporation, a wholly owned subsidiary of Lockheed Martin Corporation, for the U.S. Department of Energy's National Nuclear Security Administration under contract DE-AC04-94AL85000.

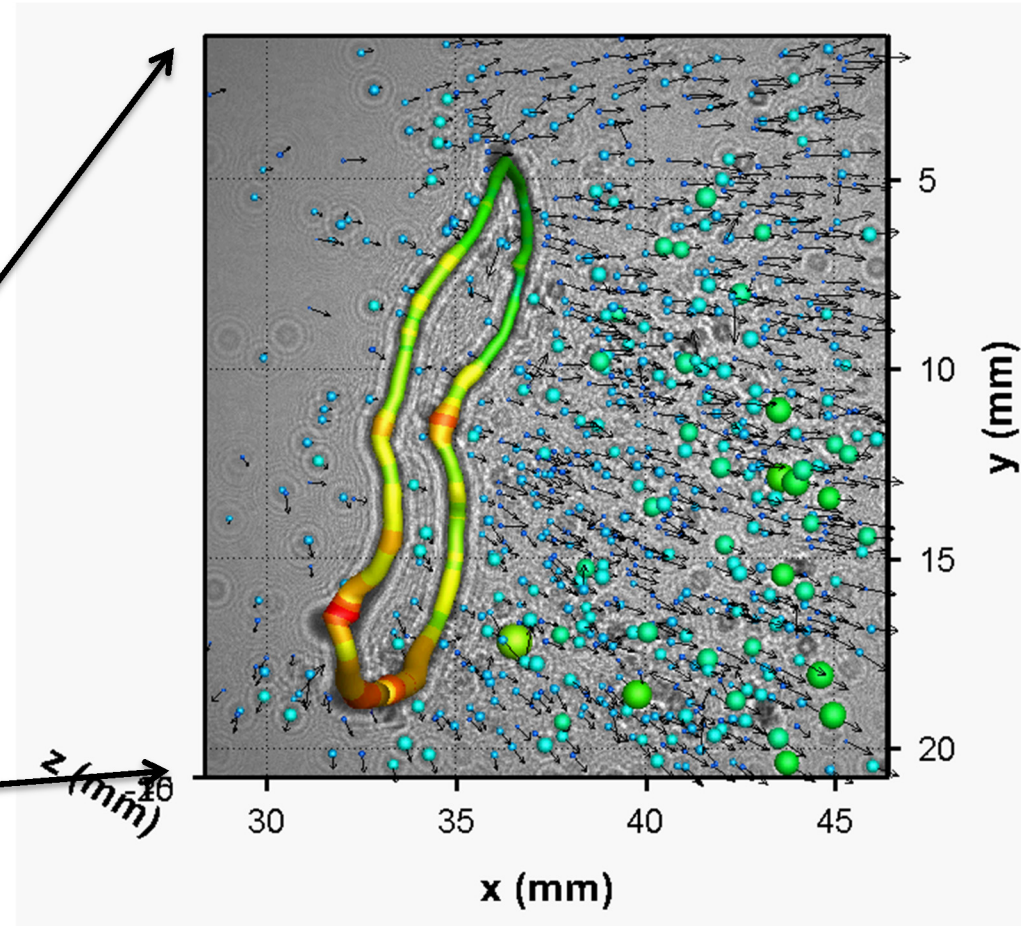
Motivation: 3D imaging for a 3D world

Widely available 2D imaging or point-wise measurement techniques are often insufficient to resolve 3D flow phenomena

- Repetition needed to capture spatial statistics



high-speed video of an ethanol drop in an air-stream

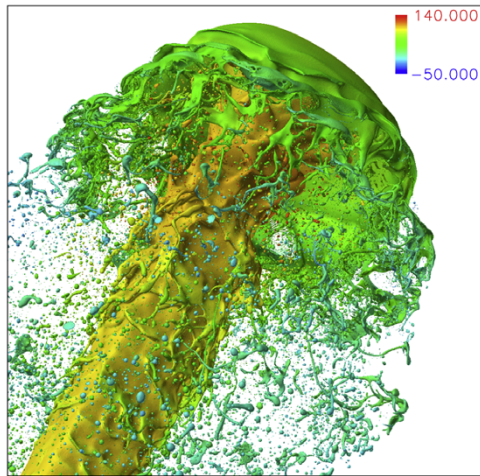


digital holographic measurement
(Gao, Guildenbecher et al, 2013, *Opt. Lett.*)

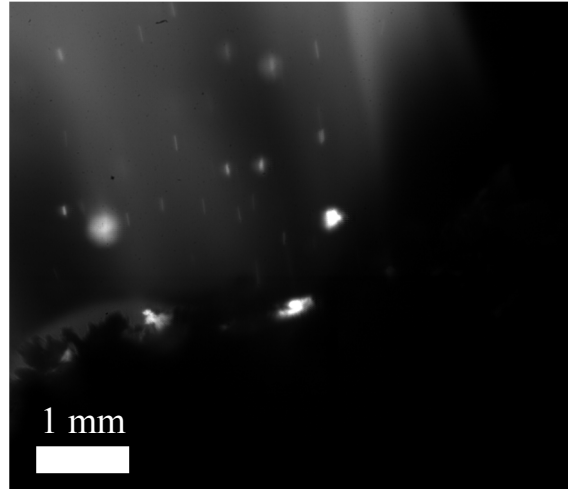
Holography is an optical technique to record and reconstruct a 3D light field

Motivation: Single-shot particle statistics

Multi-phase particle flows are often transient and highly 3D



Shinjo and Umemura, 2010,
Int. J. Multiphase Flow

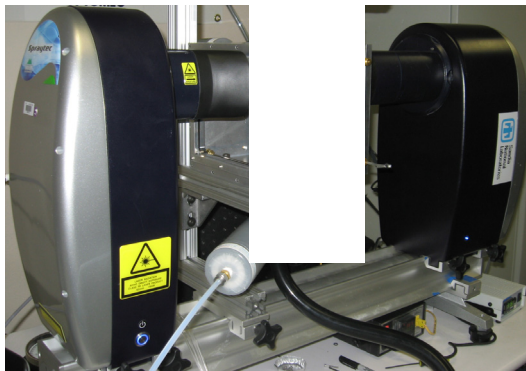


high-speed video of a burning propellant



impact of a water drop on a thin-film.
Guildenbecher et al, 2013, *Exp. Fluids*.

Yet our diagnostics are mostly limited to 1D or 2D



laser diffraction



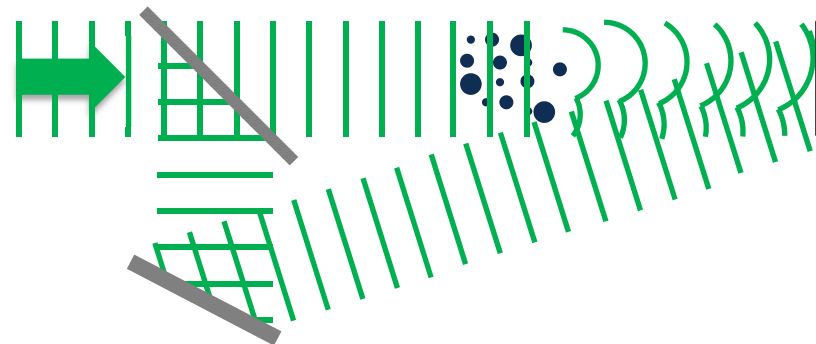
phase Doppler

Digital Holography is one potential solution

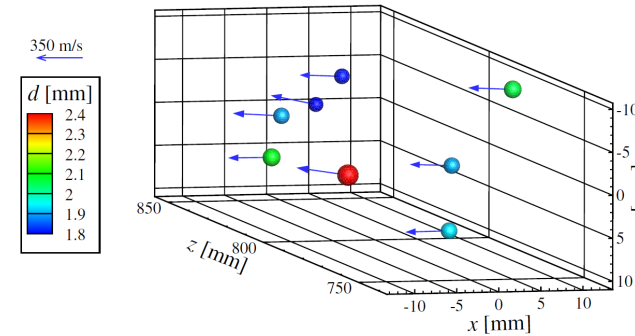
- Large 3D measurement volumes → 1000s of particles from single-shot experiments
- High-speed recording for transient dynamics
- Direct imaging of non-spherical particles

Outline for talk

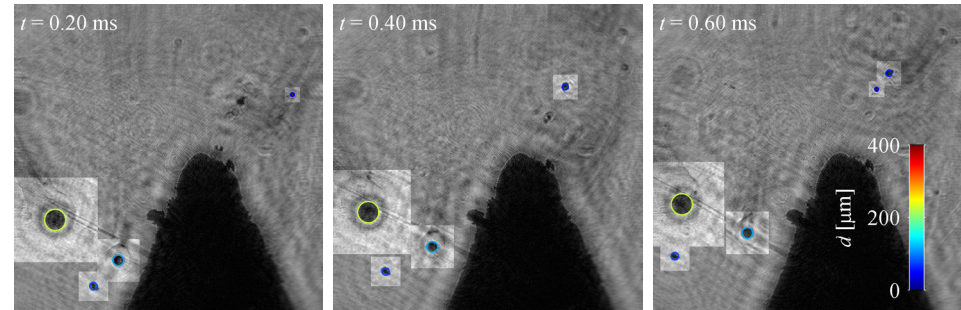
Introduction to holography and the “digital revolution”



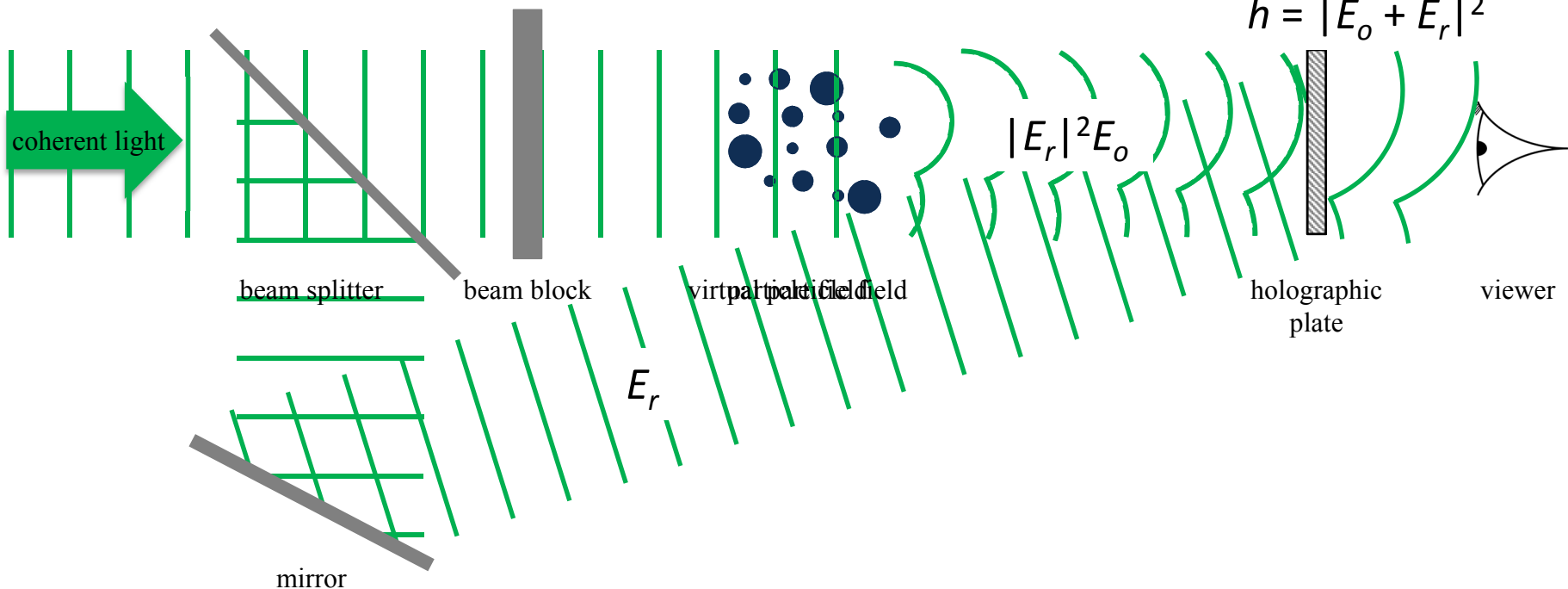
Particle measurements



Recent advancements



What is holography?



Optical method first proposed by Gabor in 1948

1. Coherent light diffracted by particle field forms the object wave, E_o
2. Interference with a reference wave, E_r , forms the hologram: $h = |E_o + E_r|^2$
3. Reconstruction with E_r forms virtual images at original particle locations

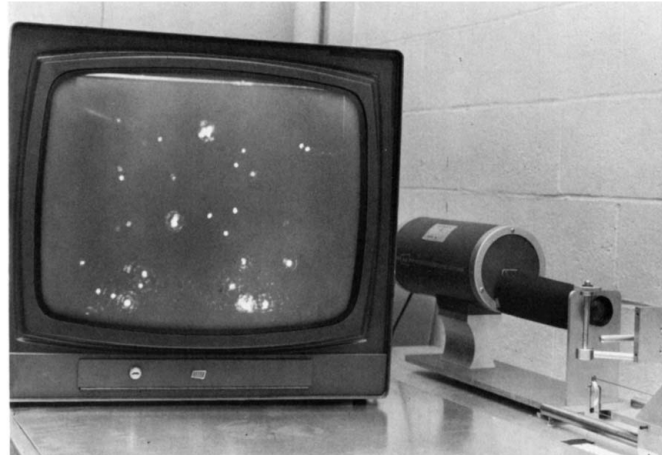
$$h \cdot E_r = \underbrace{(|E_o|^2 + |E_r|^2)E_r}_{\text{DC term}} + \underbrace{|E_r|^2 E_o}_{\text{virtual image}} + \underbrace{E_r^2 E_o^*}_{\text{real image}}$$

Analog holography

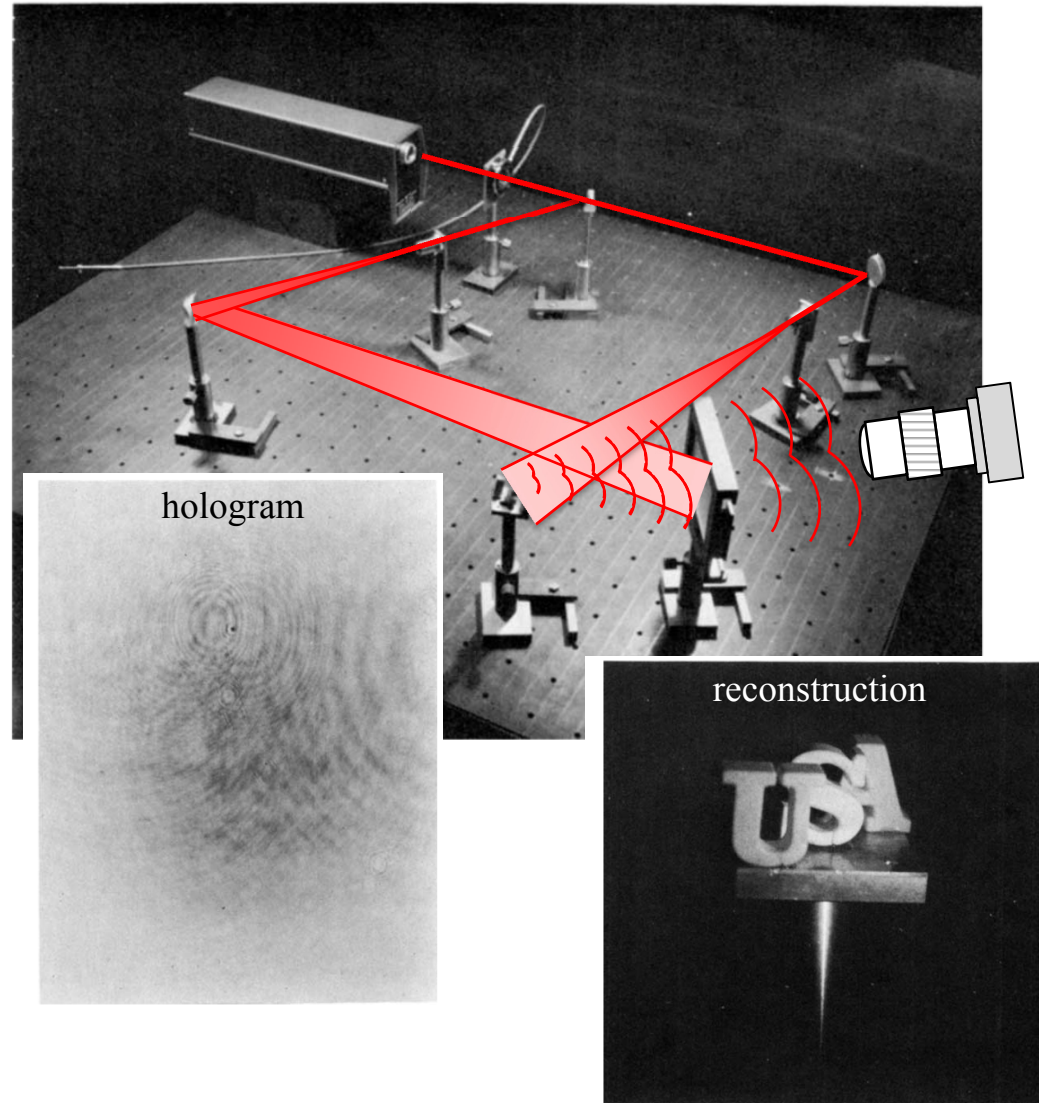
Applications of holography took off with invention of the laser in 1960

Challenges:

- Darkroom needed to process the hologram
- Limited temporal resolution
- Manual post processing

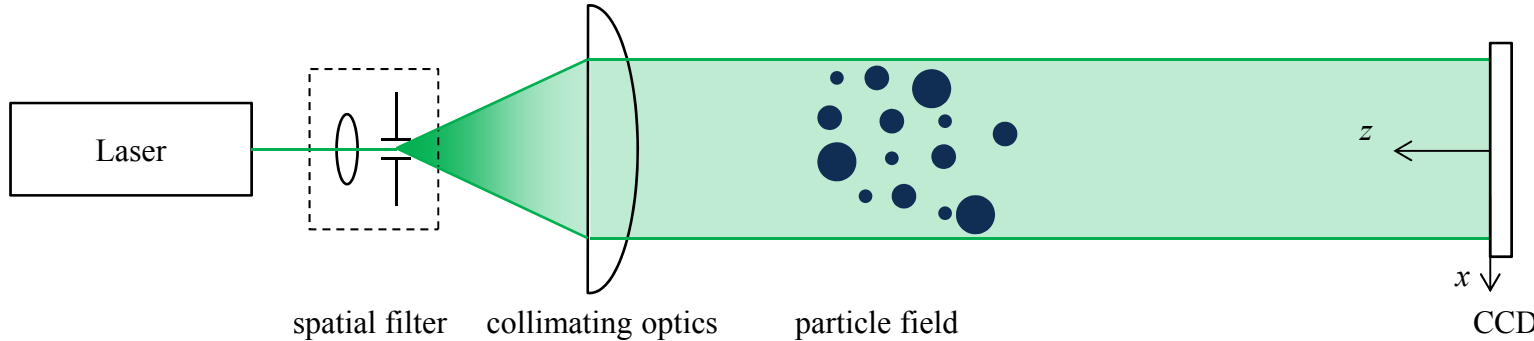


Thompson et al, 1967, *Appl. Opt.*



Collier et al, 1971, *Optical Holography*

Digital in-line holography (DIH)



Holographic plate and wet-chemical processing replaced with digital sensor

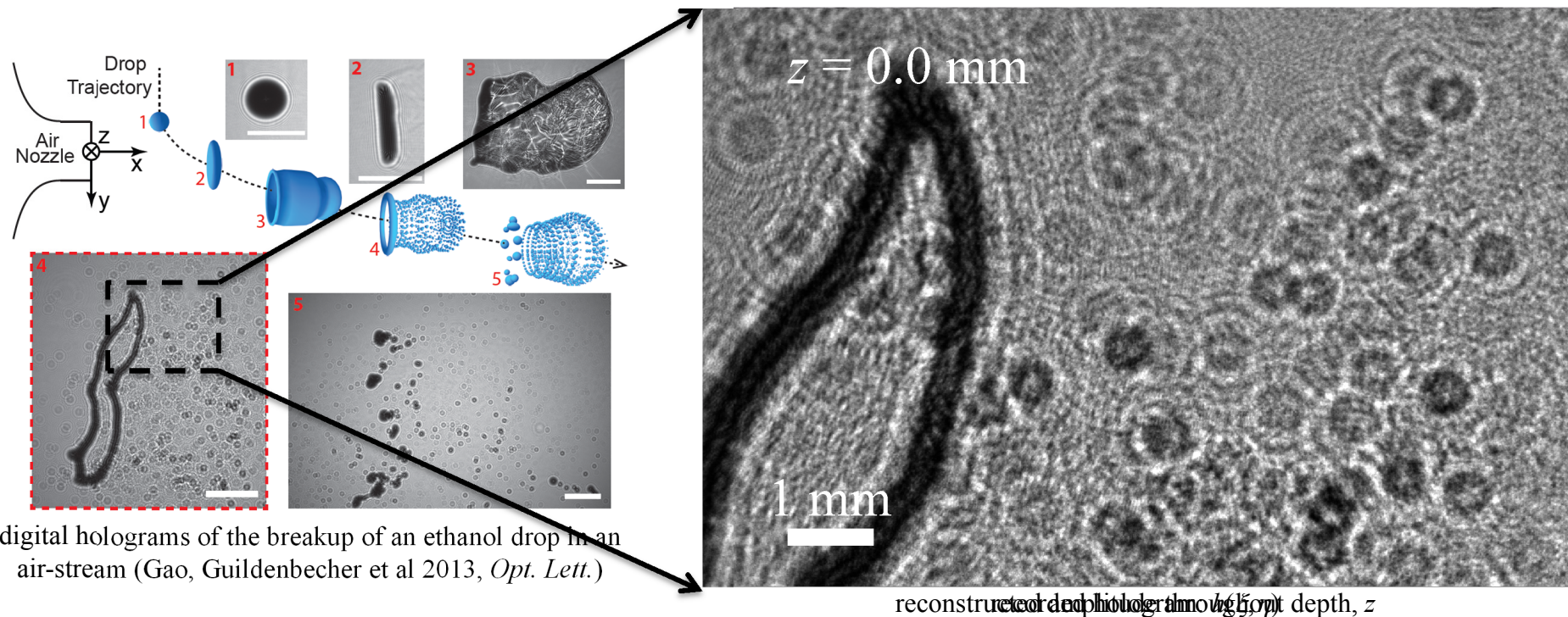
- First proposed by Schnars and Jüptner in '90s
- Advantages: (1) no darkroom, (2) temporal resolution is straight forward, (3) results can be numerically refocused and post-processed
- Challenge: Resolution of digital sensors (order 100 line pairs/mm) is much less than resolution of photographic emulsions (order 5,000 line pairs/mm)
 - For suitable off axis angles, θ , the fringe frequency, f , is typically too large to resolve with digital sensors ($f = 2\sin(\theta/2)/\lambda$)
 - Rather, the in-line configuration ($\theta = 0$) is typically utilized

Numerical refocusing

Light propagation in a non-absorbing, constant index of refraction medium is described by the diffraction integral equation:

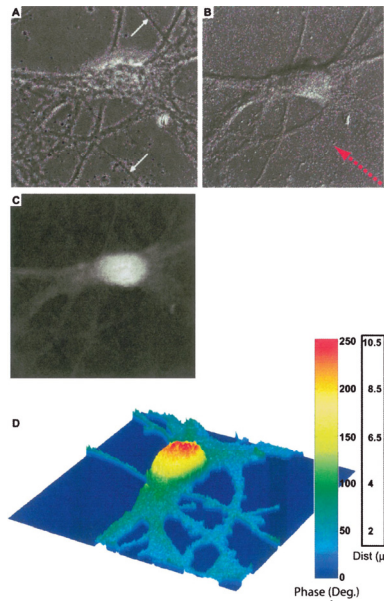
$$E(x, y, z) = \frac{1}{\lambda} \iint E(\xi, \eta, z=0) \frac{e^{-jkr}}{r} d\xi d\eta \quad \text{where: } r = \sqrt{(\xi - x)^2 + (\eta - y)^2 + z^2}$$

- $E(\xi, \eta, 0) \equiv$ complex amplitude at hologram plane = $h(\xi, \eta) \cdot E_r^*$
- $E(x, y, z) \equiv$ refocused complex amplitude at optical depth z



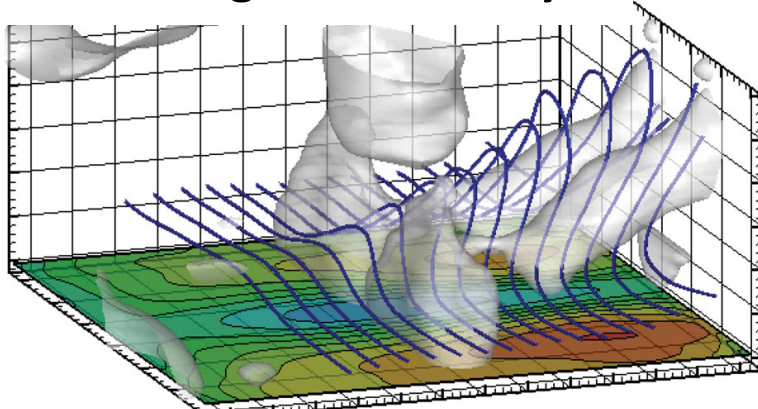
DIH in the literature

Microscopy



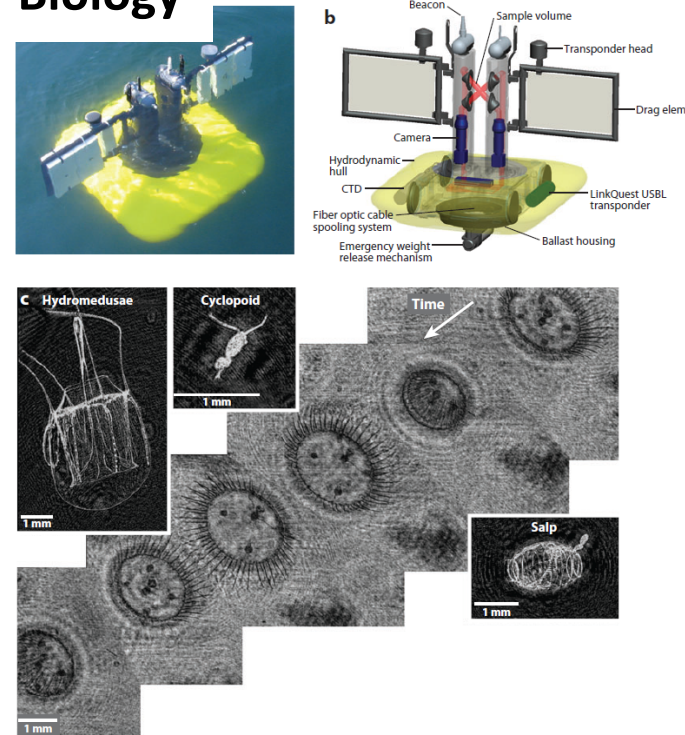
Marquet et al 2005, *Opt. Lett.*

Particle Image Velocimetry



Sheng et al 2009, *J. Fluid Mech.*

Biology

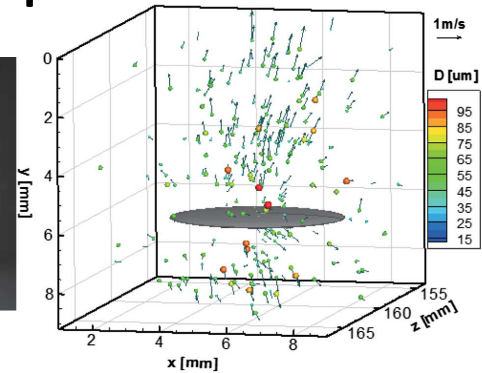


Katz and Sheng 2010, *Annu. Rev. Fluid Mech.*

Multiphase Flows



Yao et al 2015, *Appl Opt.*



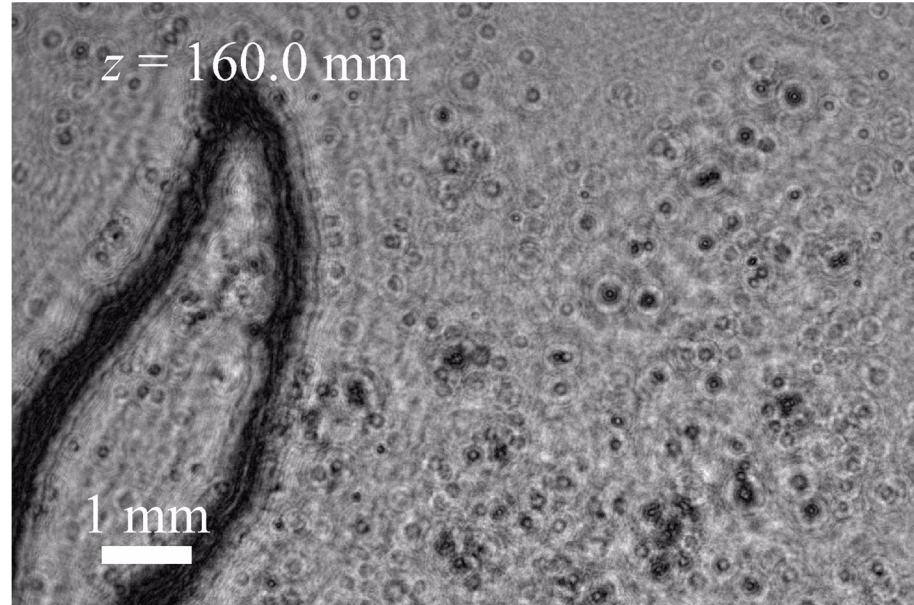
Particle measurements

Data processing

Acquisition and refocusing of a digital hologram is relatively straightforward.

However...

For quantitative measurements, methods are required to locate and measure particles.



Challenge: depth-of-focus problem

The spatial extent of the diffraction pattern limits the angular aperture, Ω , from which a particle is effectively reconstructed (Meng et al, 2004, *Meas. Sci. Technol.*)

- From the central diffraction lobe $\rightarrow \Omega \approx 2\lambda/d$
- Using the traditional definition of depth-of-focus, δ , based on change of intensity within the particle center $\rightarrow \delta \approx 4\lambda/\Omega^2$
- Therefore: for in-line holography, $\delta \approx d^2/\lambda$
 - Example: $d = 300 \mu\text{m}$, $\lambda = 532 \text{ nm} \rightarrow \delta \approx 170 \text{ mm}!$

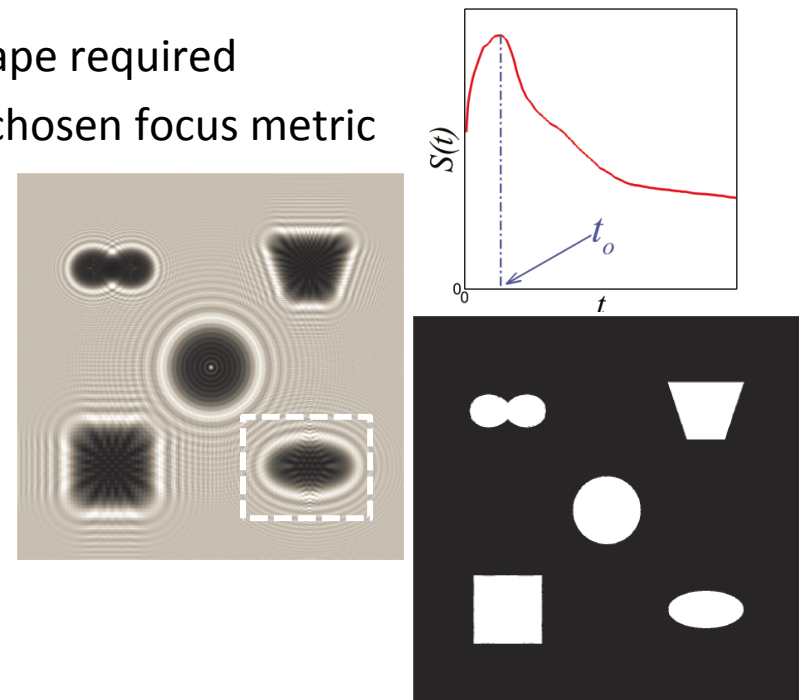
Data processing

Literature contains two basic methods to find the focal plane:

1. Fit a model to the observed diffraction patterns (inverse method)
 - Generally accurate with small depth uncertainty
 - Limited to objects with known diffraction patterns (spheres)
2. Reconstruct the amplitude (or intensity) throughout depth and apply a focus metric to find “in-focus” objects
 - No *a-priori* knowledge of particle shape required
 - Accuracy is a strong function of the chosen focus metric

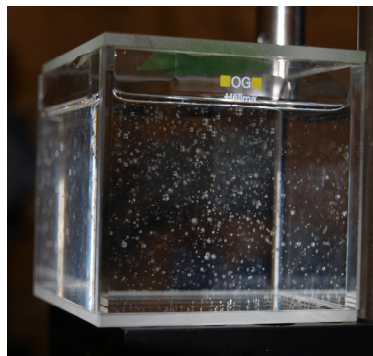
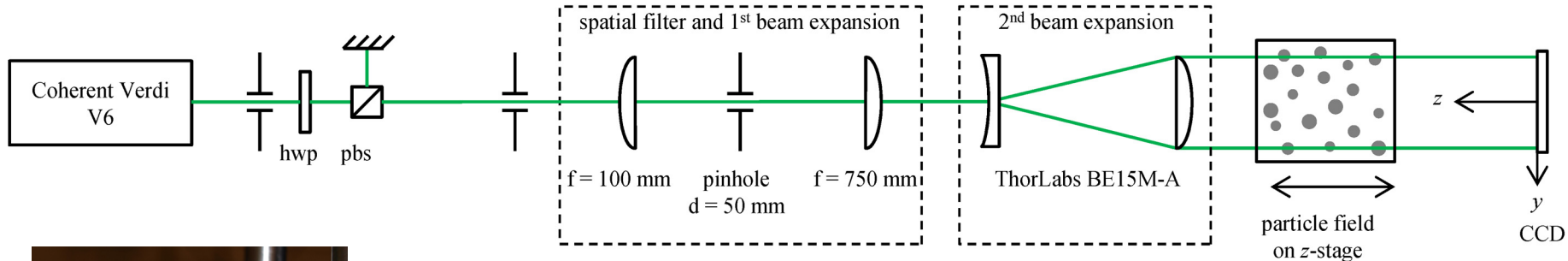
Hybrid method:

- Focus metric is a combination of amplitude minimization and edge sharpness maximization
 - Details in Guildenbecher et al 2013, *Appl. Opt.*; Gao et al 2013, *Opt. Express*; Gao et al 2014, *Appl. Opt.*



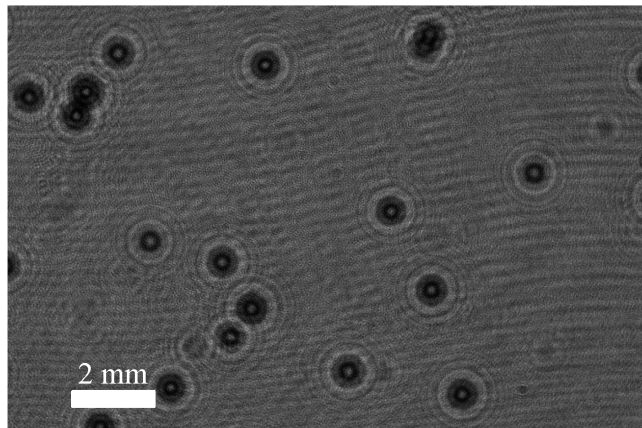
Gao et al 2014, *Appl. Opt.*

Experimental validation

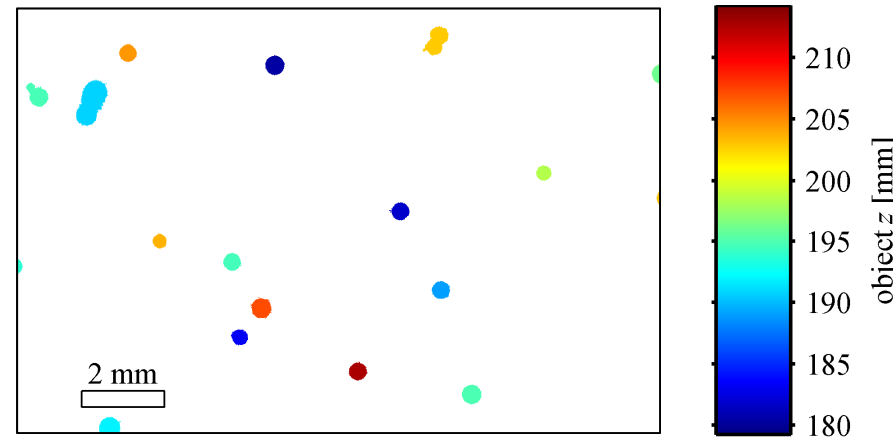


particle field

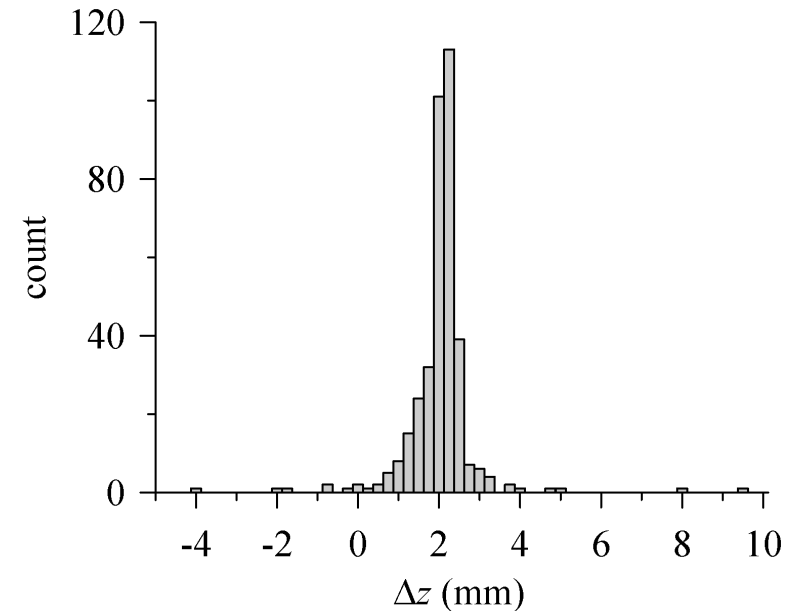
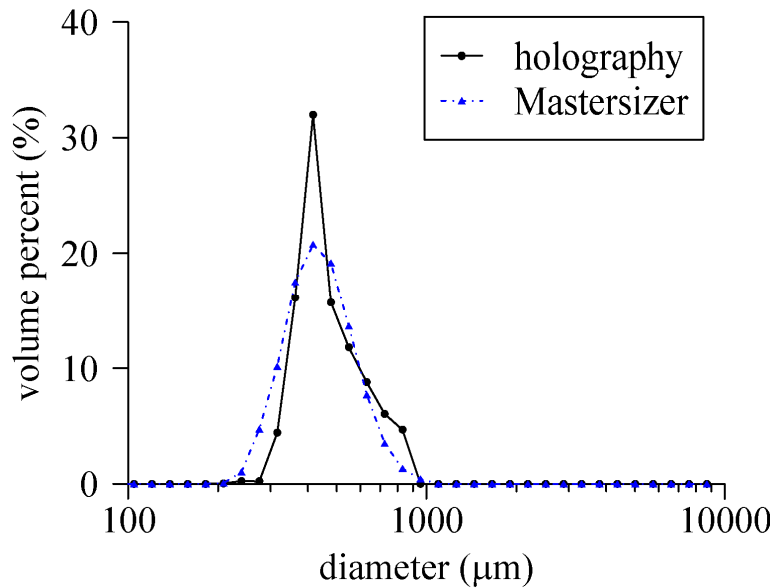
- Quasi-stationary particle field
 - Polystyrene beads ($\bar{d} \approx 465 \mu\text{m}$) in 10,000 cSt silicone oil
 - Settling velocity $\approx 0.8 \mu\text{m/s}$
- Multiple holograms recorded, displacing the particle field 2 mm in the z-direction between each acquisition



hologram



Experimental validation



Diameter measured from area of the detected 2D morphology

- Actual mass median diameter = 465 μm
- Measured mass median diameter = 474 μm
 - Error of 2.0% with respect to actual value

Displacement found by particle matching between successive holograms

- Actual displacement = 2.0 mm
- Mean detected displacement = 1.91 mm \pm 0.81 mm
- Standard deviation of 1.74 times mean diameter

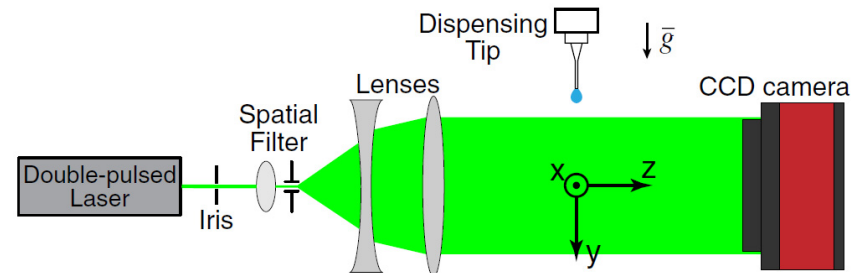
Aerodynamic drop fragmentation

Experimental configuration: Double-pulsed laser and imaging hardware as typically used in PIV

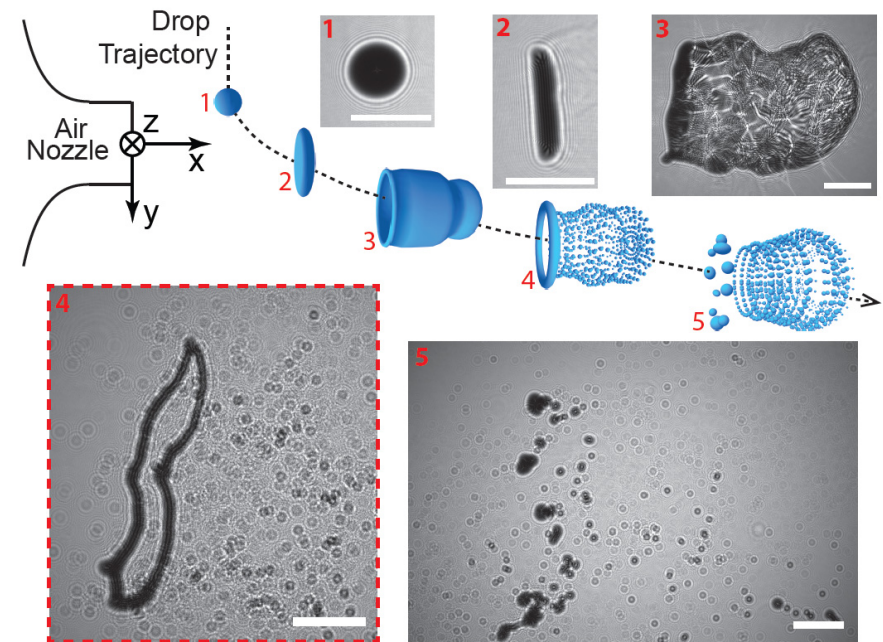
- $\lambda = 532$ nm, 5 ns pulselength
- Interline transfer CCD (4008×2672 , 9 μm pixel pitch)
- Temporal separation, $\Delta t = 62$ μs , determined by laser timing

Note: without a separate reference wave, coherence length requirements in DIH are greatly relaxed.

- Expensive injection seeders are not always needed
- Faster lasers (ps or fs) can be used with some advantages (e.g. Nicolas et al 2007, *Opt. Express*)



Optical configuration (Gao, Guildenbecher et al 2013, *Opt. Lett.*)

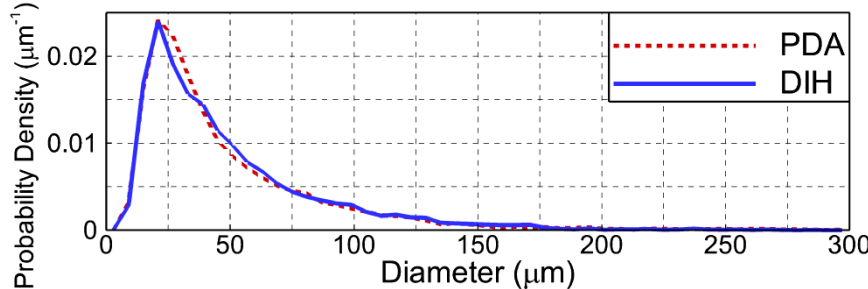


digital holograms of the breakup of an ethanol drop in an air-stream (Gao, Guildenbecher et al 2013, *Opt. Lett.*)

Aerodynamic drop fragmentation

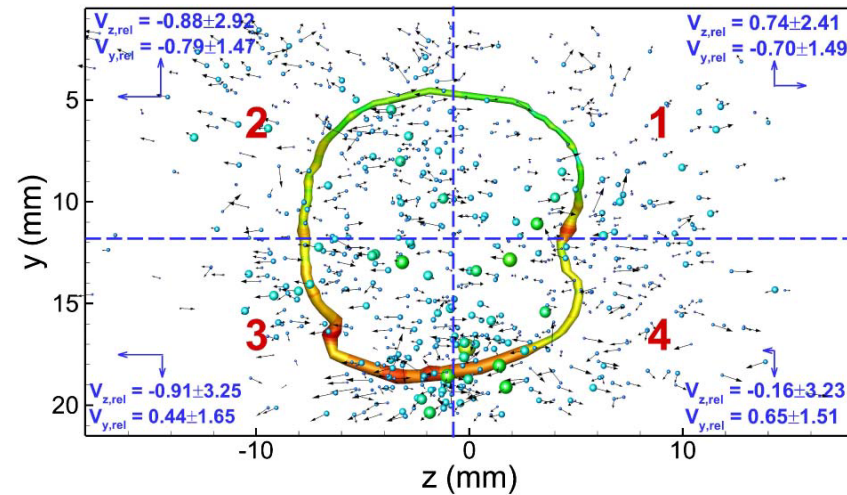
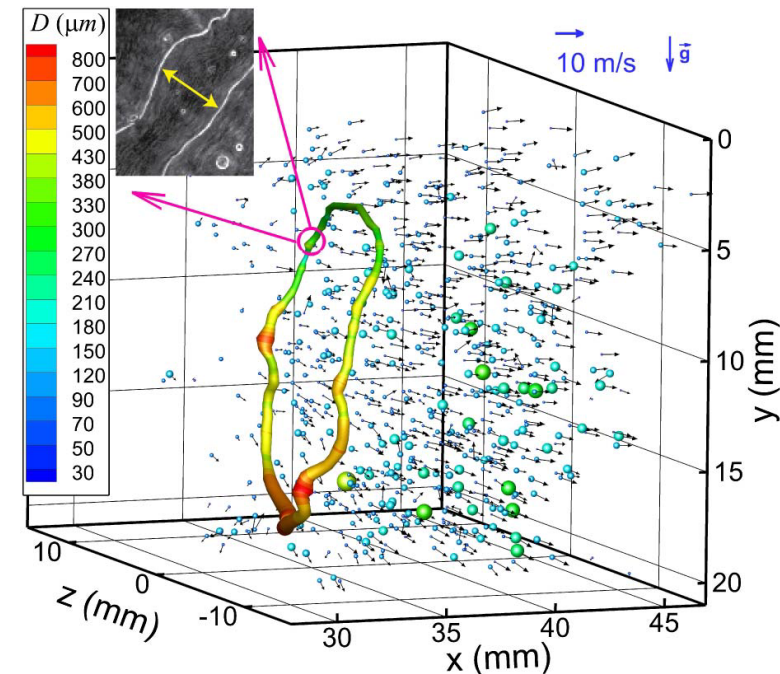
Secondary drop sizes/positions extracted by the hybrid method

- Comparison with phase Doppler anemometer (PDA) data confirms accuracy of measured sizes



Ring measured from z-location of maximum image gradient

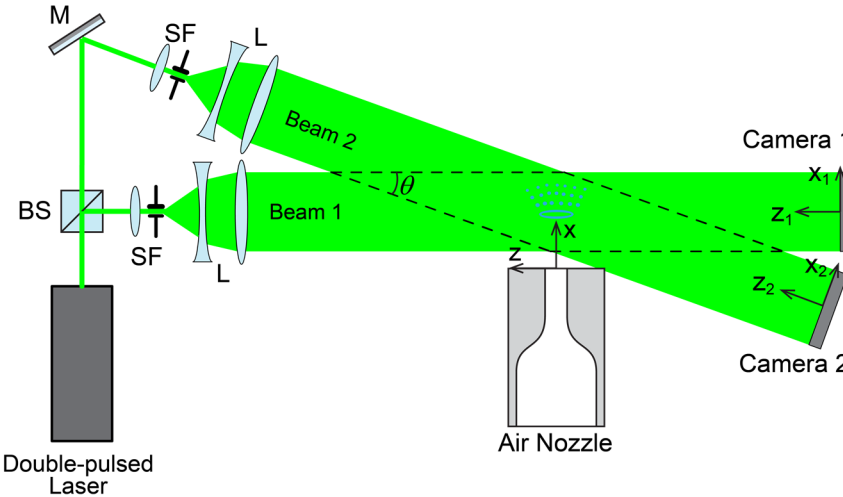
- Total volume of ring + secondary drops is within 2.2% of the initial volume



Aerodynamic drop fragmentation

Velocimetry suffers from uncertainty in the out-of-plane (z) position

- A stereo-view configuration is one solution

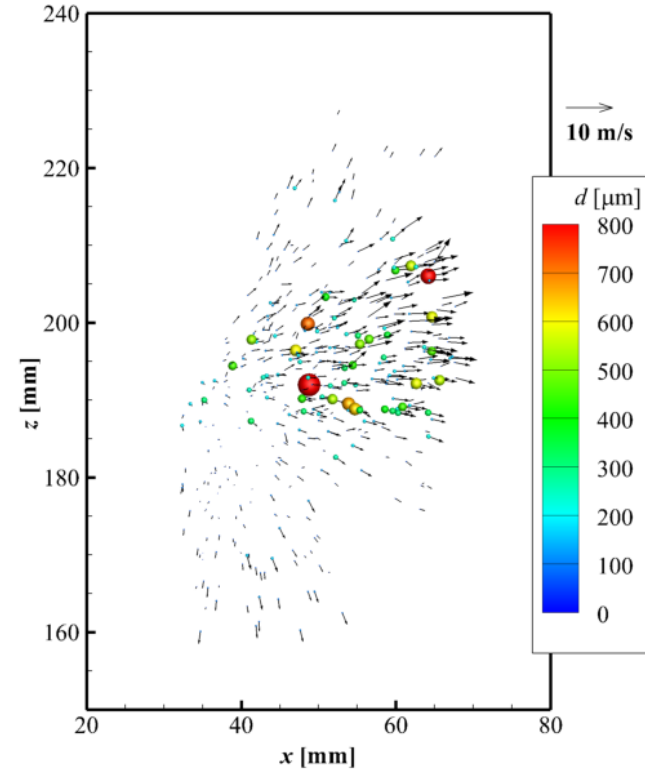
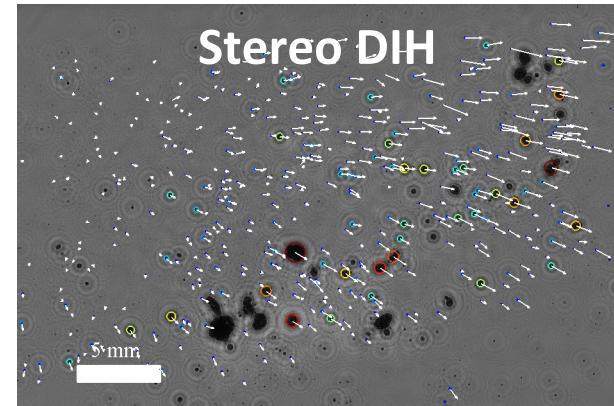


Advantages:

- Improved z-uncertainty
- Eliminates false particle size and position measurements

Challenges:

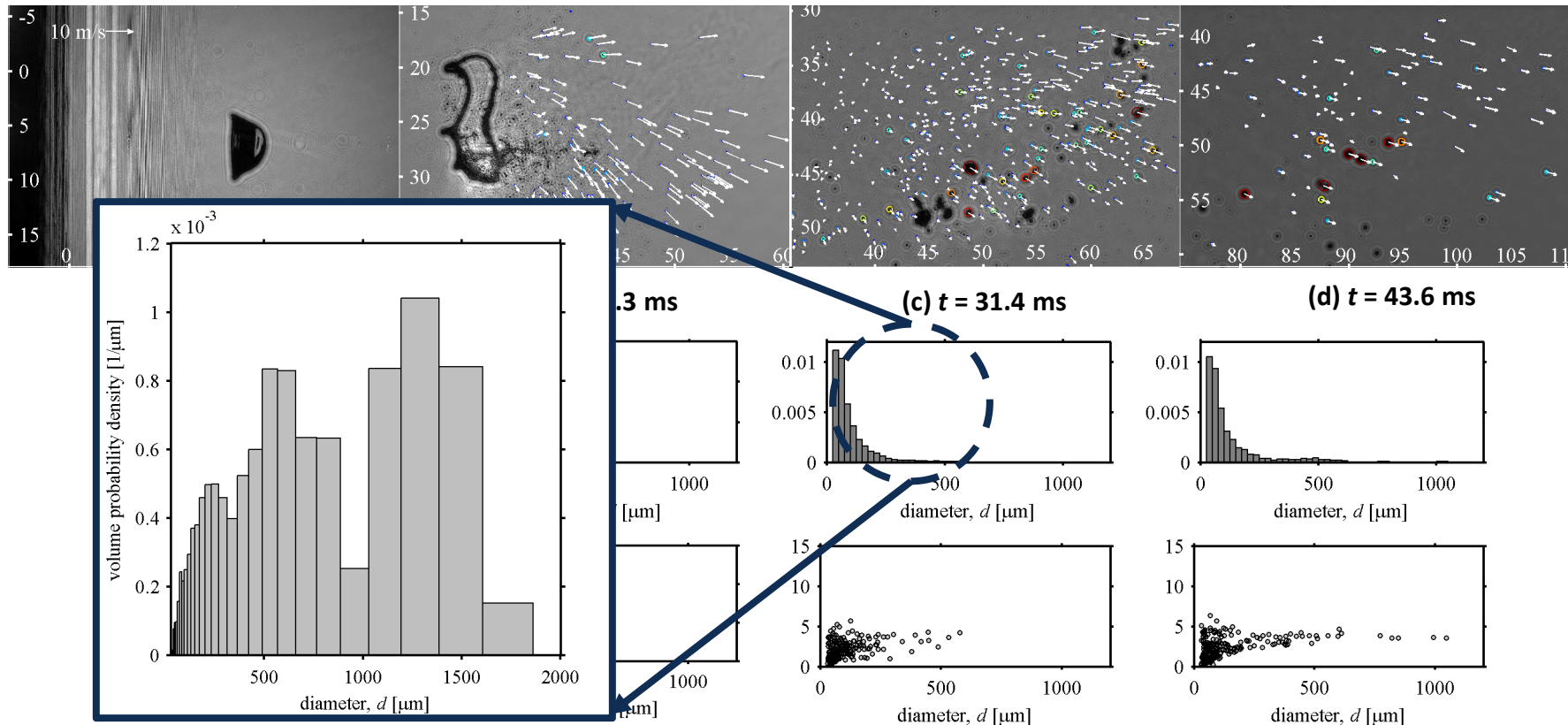
- Increased experimental complexity
- Careful calibration required



Aerodynamic drop fragmentation

Ensemble averaging of 44 realizations at each condition

- Roughly 10,000 individual drops measured per condition



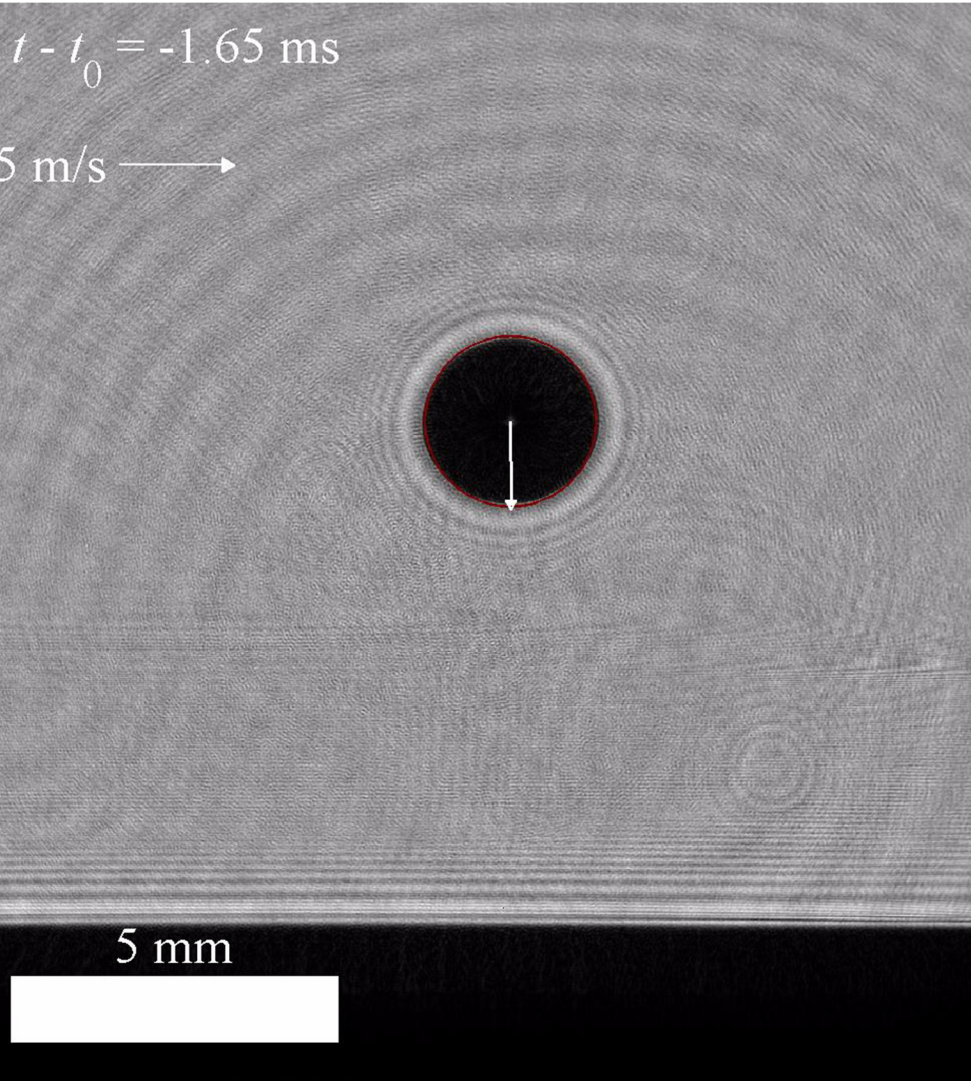
DIH is particularly advantageous for rapid quantification of particle statistics

Recent advancements

High-speed (kHz) DIH

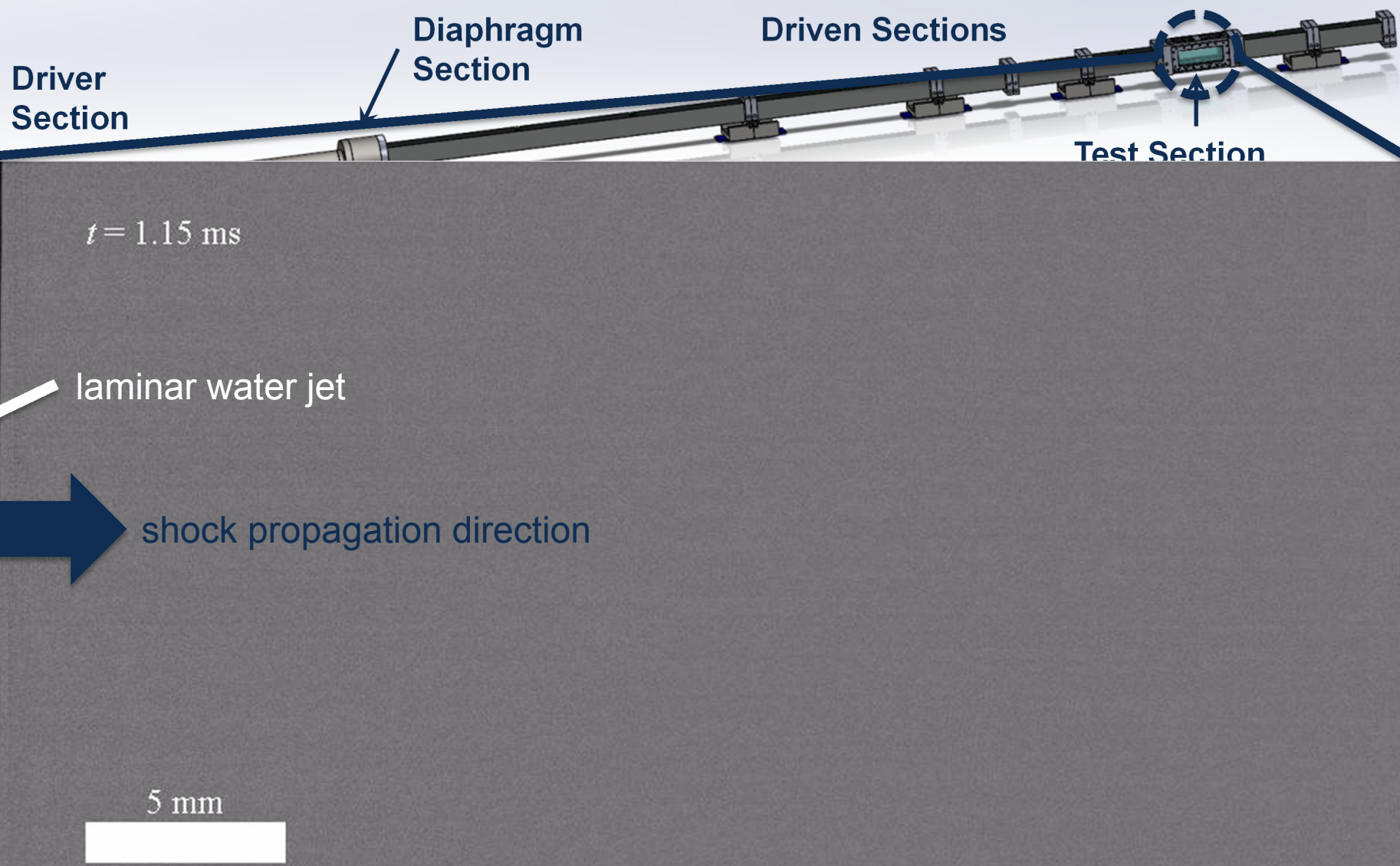
$$t - t_0 = -1.65 \text{ ms}$$

5 m/s →

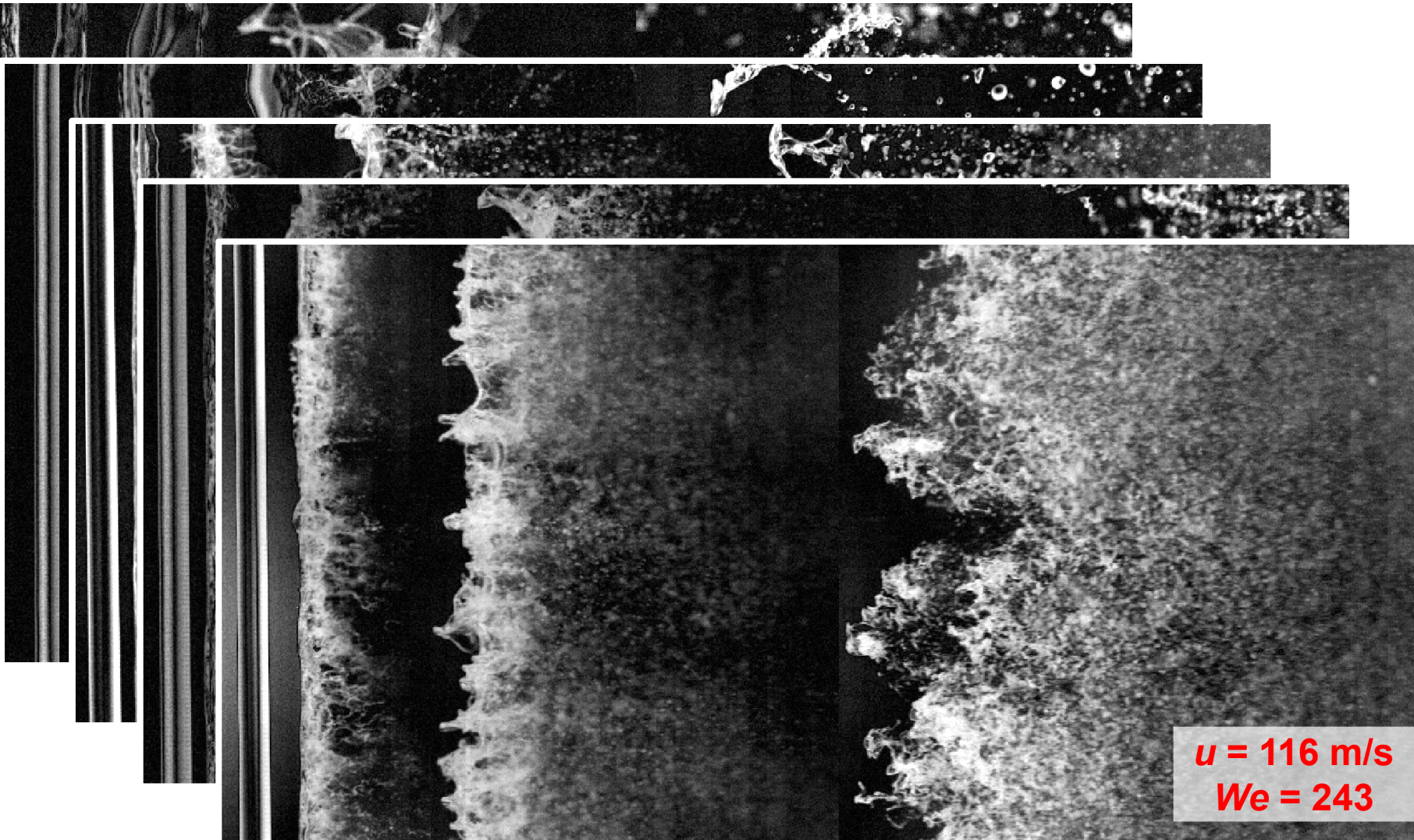


Regression based Multi-frame Tracking (RMT) allows for 3D-3C temporal measurements (Gildenbecher *et al.*, 2016, *Appl. Opt.*)

Breakup of a water jet in a shock-tube

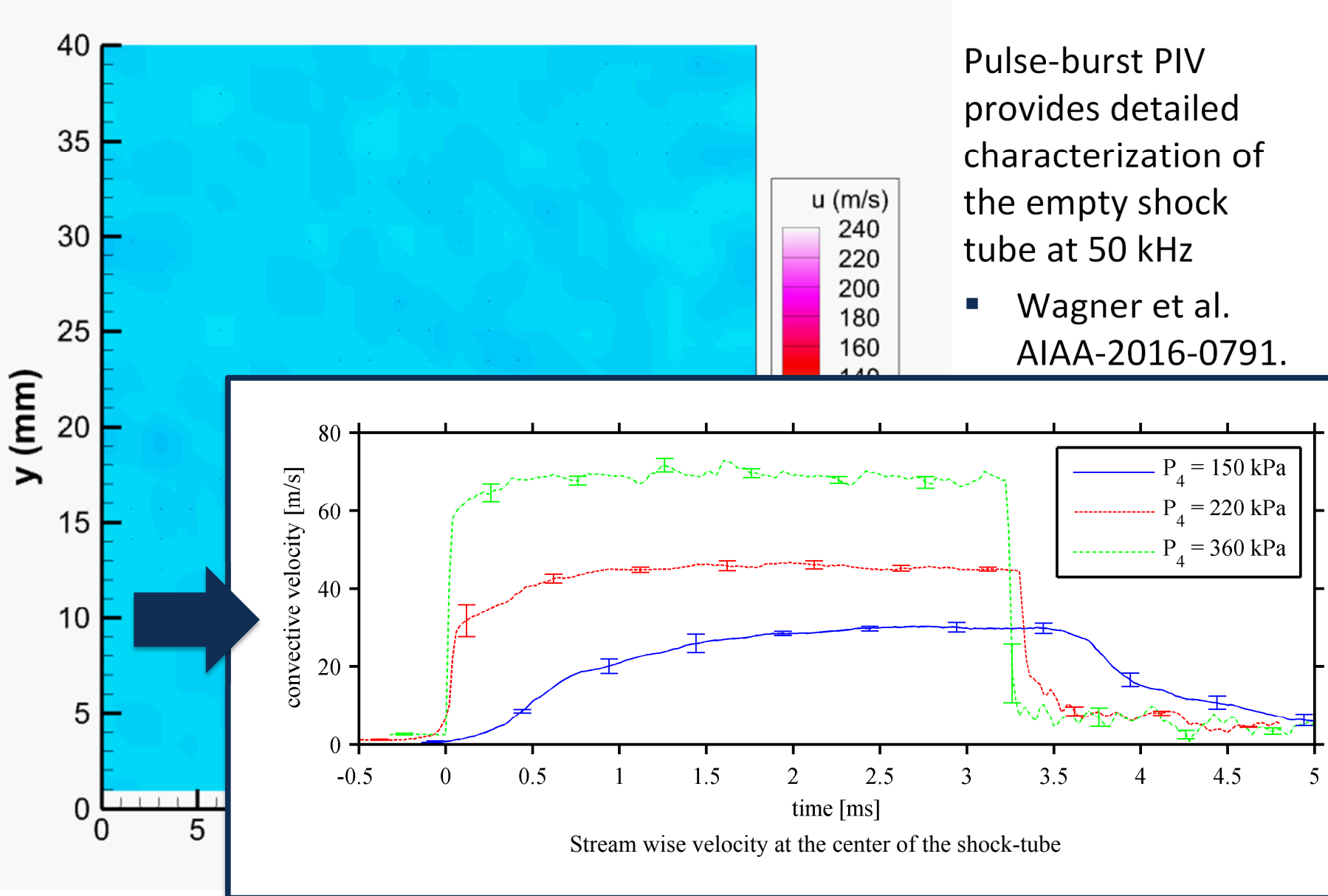


Observed breakup morphologies



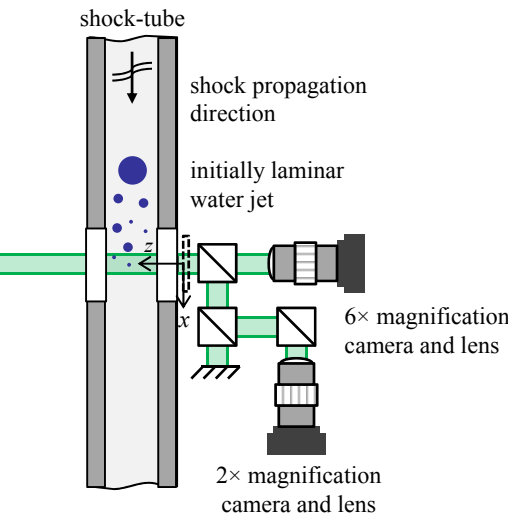
Breakup morphologies similar to those observed for isolated drops

Well characterized boundary conditions



DIH recorded at 100,000 fps

recorded hologram at $t = 1.16$ ms



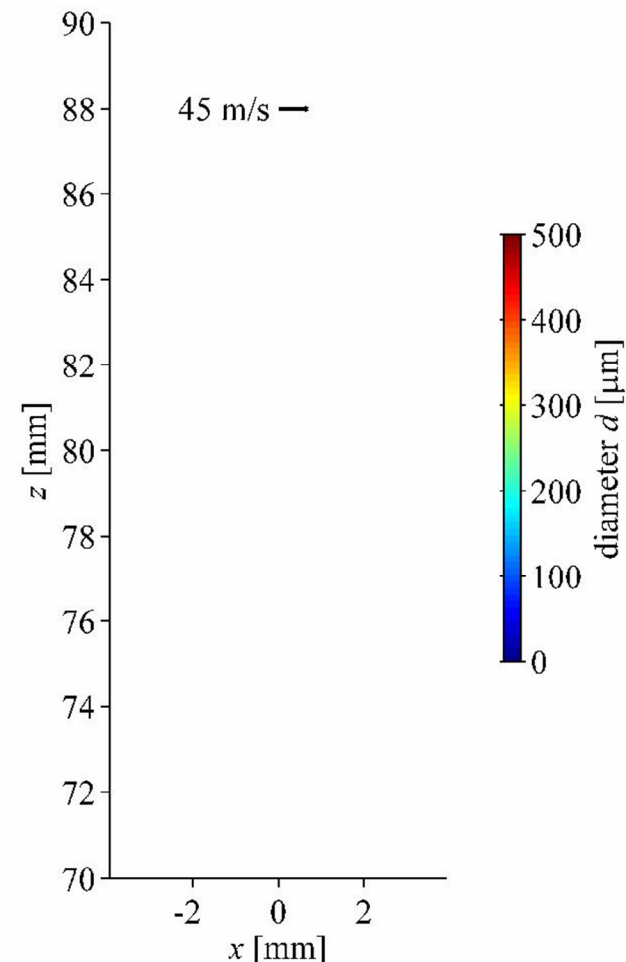
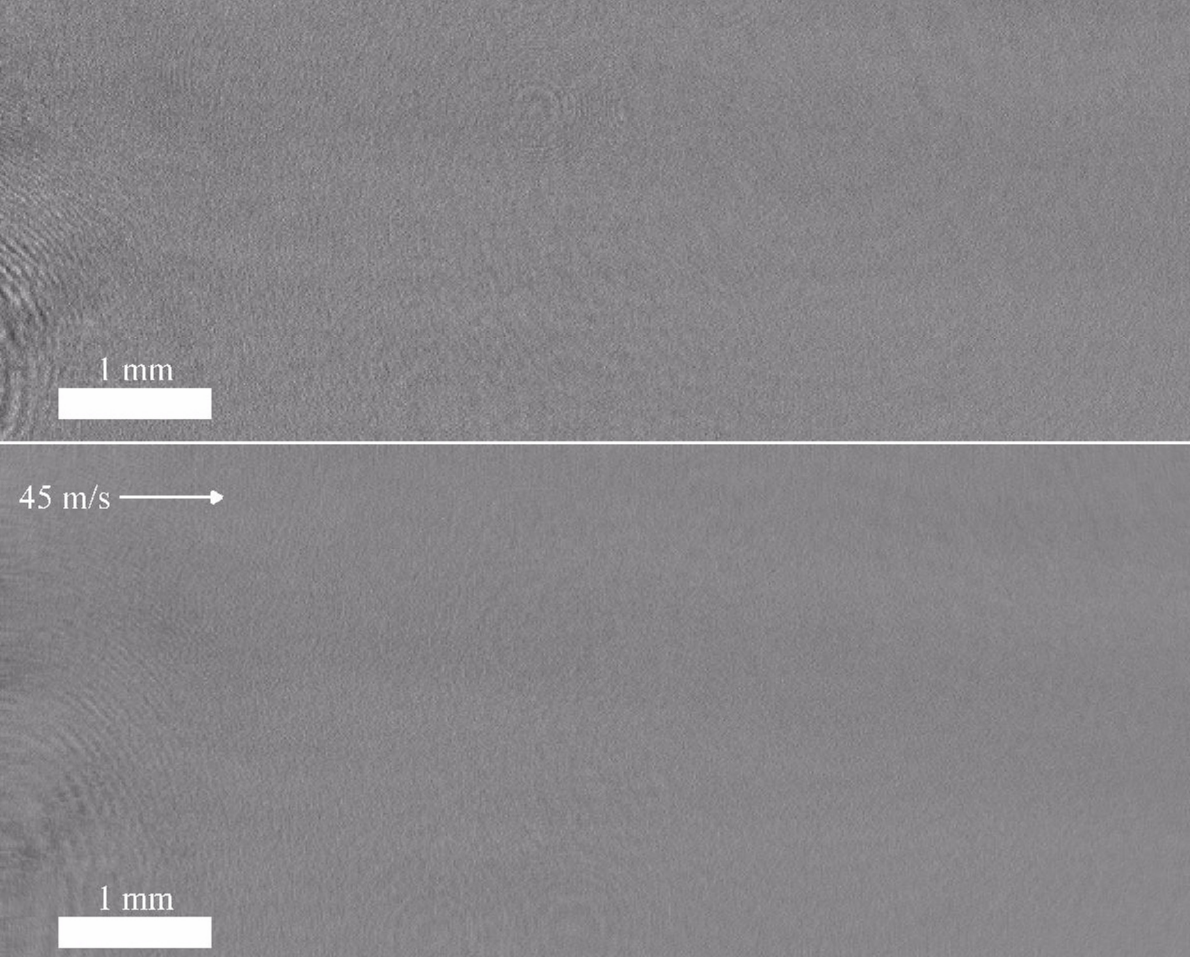
refocused to $z = 80$ mm

1 mm

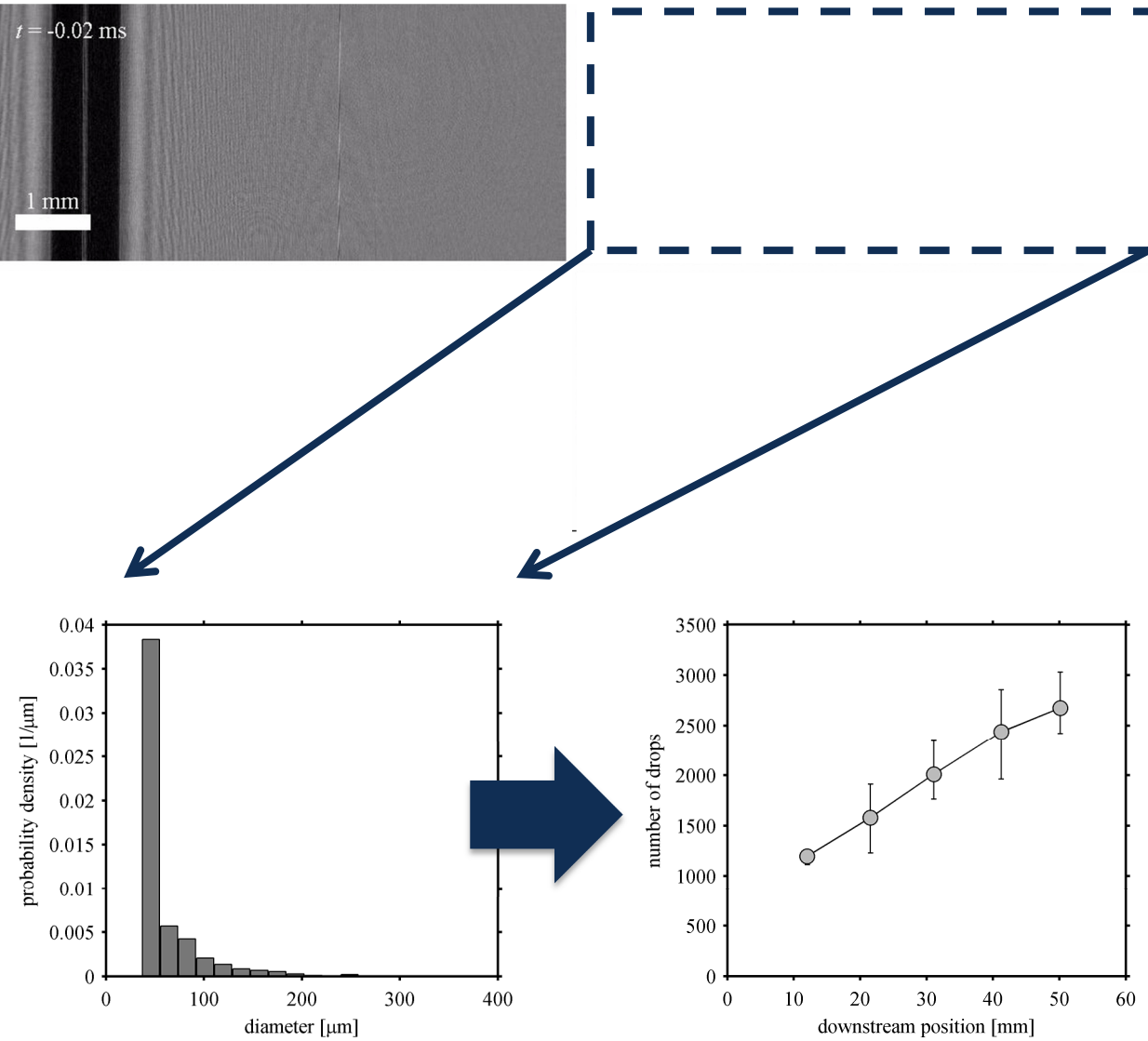
Temporally resolved, 3D particle field

Data processing similar to drop impact experiment

recorded hologram at $t = 1.29$ ms

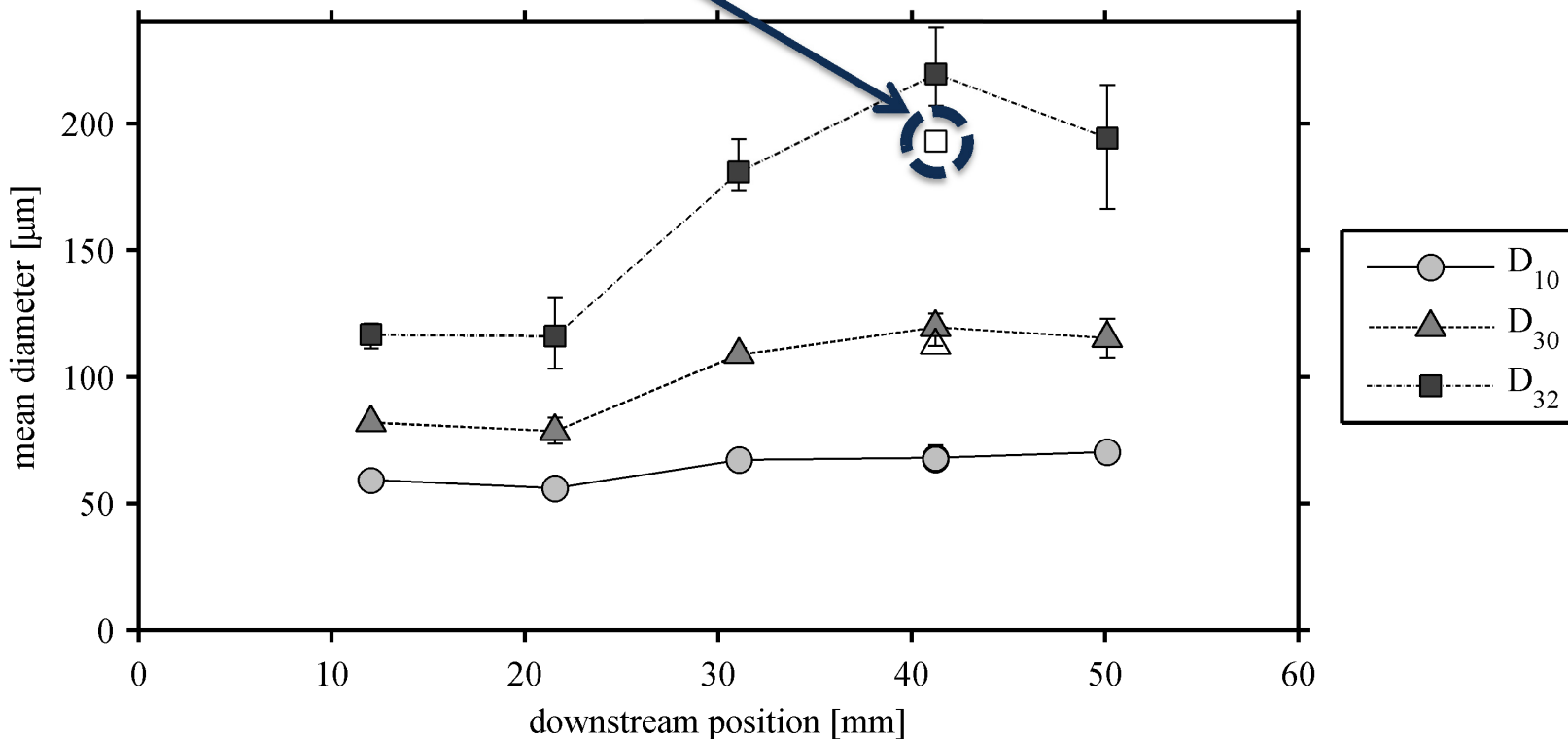
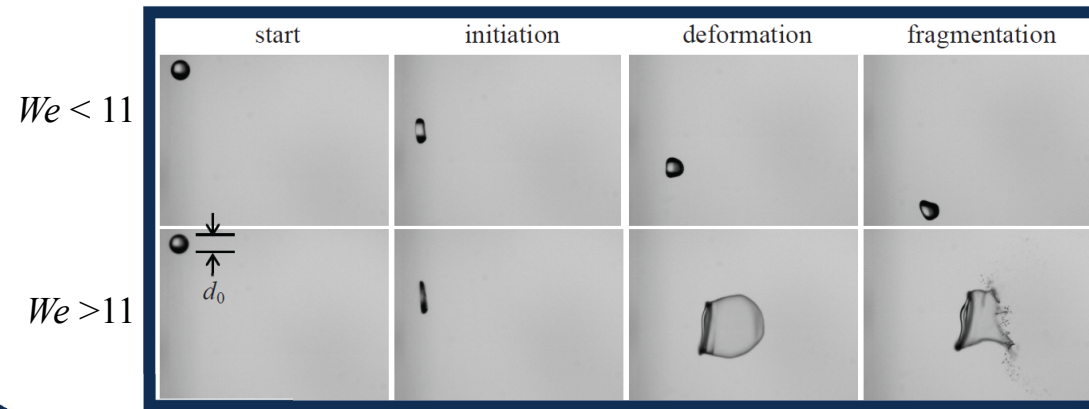


Multiple downstream fields of view



Characteristic mean diameters

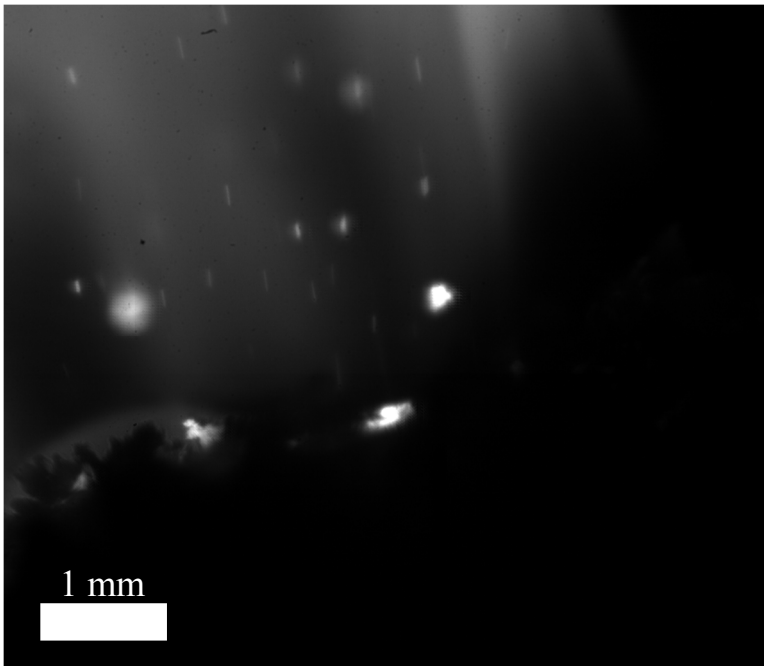
- Measured drops with relative $We > 11$ are expected to be unstable and will break apart further
- Excluding drops with $We > 11$ eliminates the unusual dip



Aluminum drop combustion in propellants

Motivation: rocket failures can lead to propellant fires

- Sandia Laboratories is interested in predicting the response of objects in this environment



high-speed video of a burning propellant

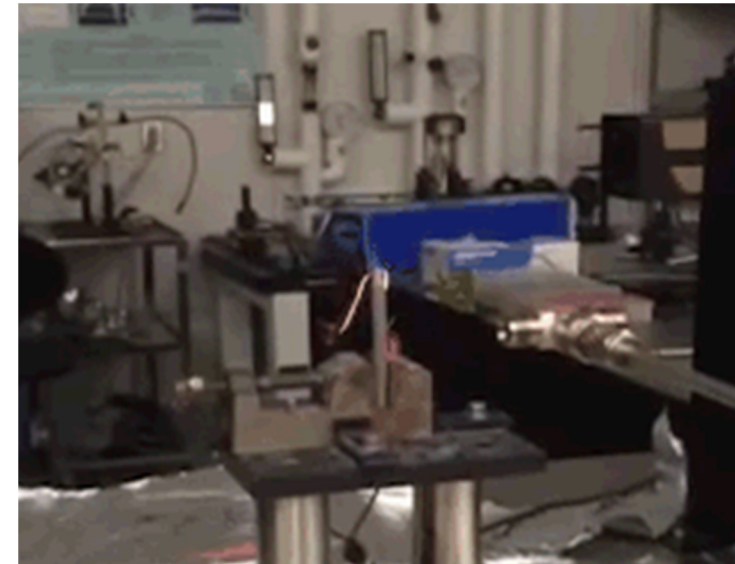
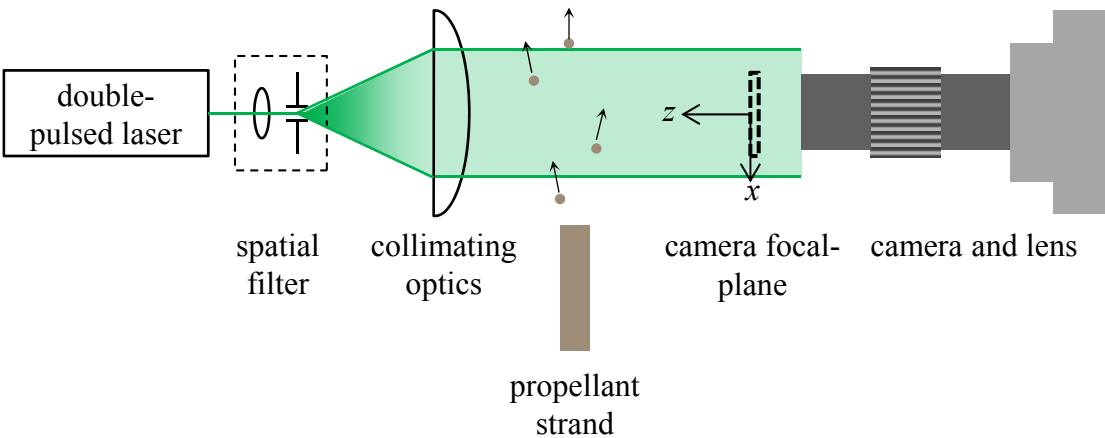


<http://www.cbsnews.com/news/rocket-crash-no-immediate-threat-to-station-but-cause-is-unknown/>

Aluminum agglomeration at the surface yields large reacting drops with high damage potential

- Prediction requires knowledge of particle *size, velocity, and temperature*

Aluminum drop combustion in propellants



propellant in the test fixture

Propellant: solid-rocket propellant pressed into a pencil size strand

- Combusts from the top surface down, ejecting molten aluminum particles traveling a few m/s

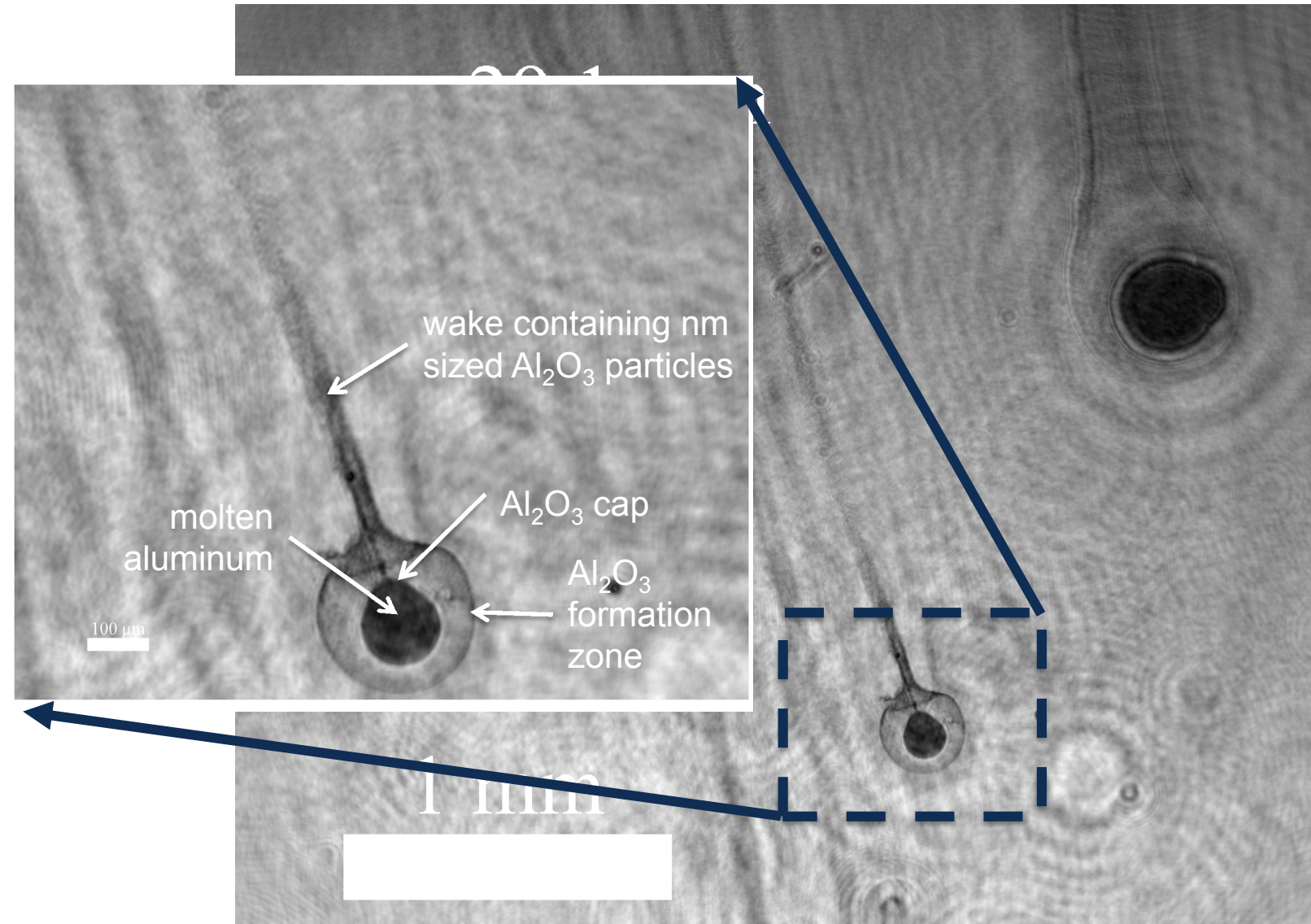
Laser: Continuum Minilite Nd:YAG, 532 nm wavelength, 5 ns pulse duration

Camera: sCMOS from LaVision at 15Hz

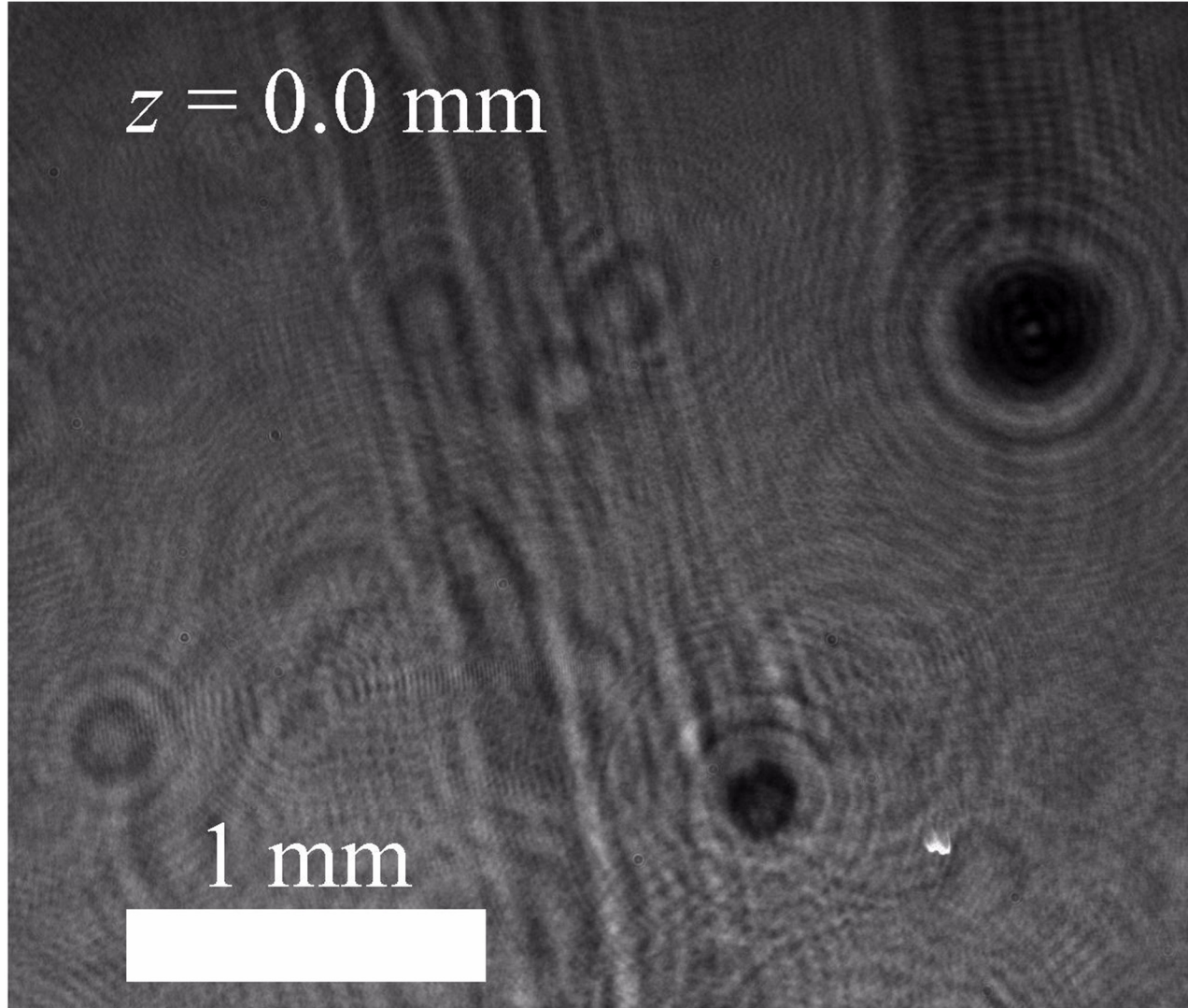
Lens: Infinity K2 long distance microscope with CF-4 objective

- ~ 6X magnification

Aluminum drop combustion in propellants



Aluminum drop combustion in propellants



Algorithms automatically measure unique features of burning aluminum

Aluminum drop combustion in propellants

Three strand burns \rightarrow 5594 images and 17496 measured drops

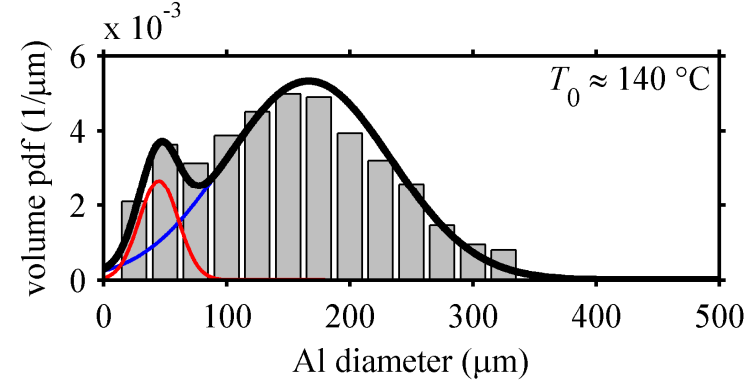
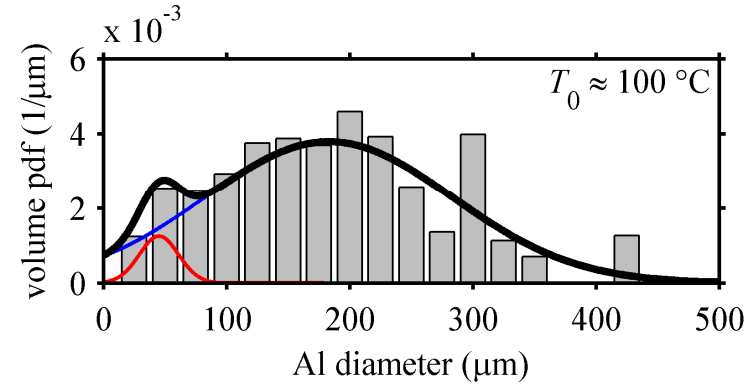
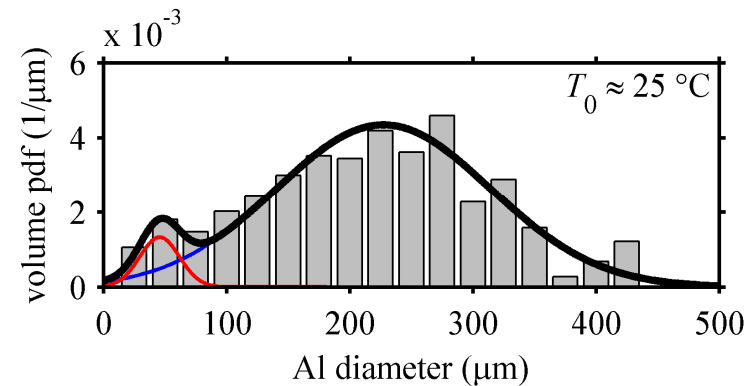
- Main peak due to agglomerated particulates
- Peak at 50 μm due to non-agglomerated particulate

Experiments repeated at higher initial temperature (faster burn rate)

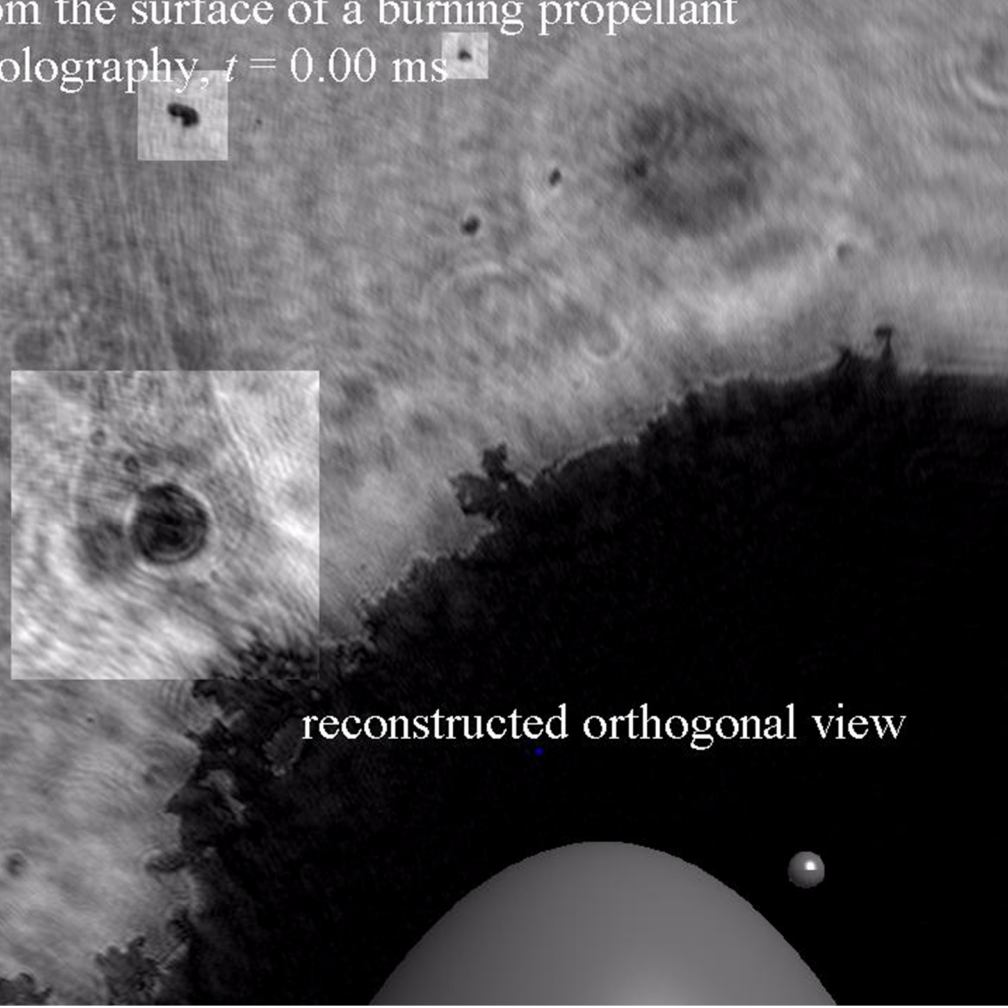
- Main peak is reduced due to decreased residence time for agglomeration
- Peak at 50 μm remains

Trend is consistent at still higher initial temperatures

- Main peak reduced further
- Peak at 50 μm remains



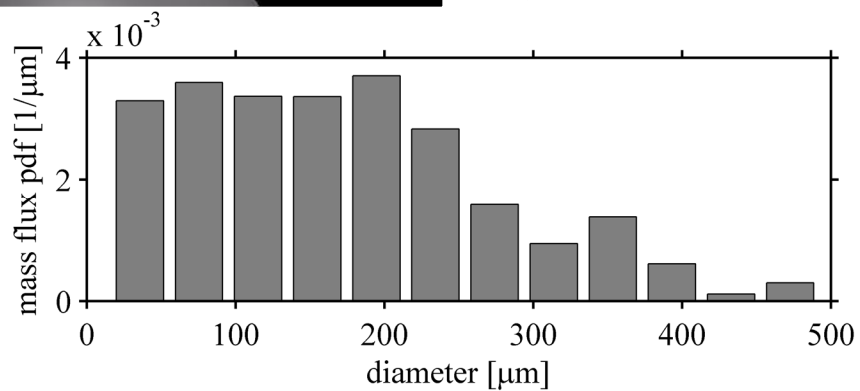
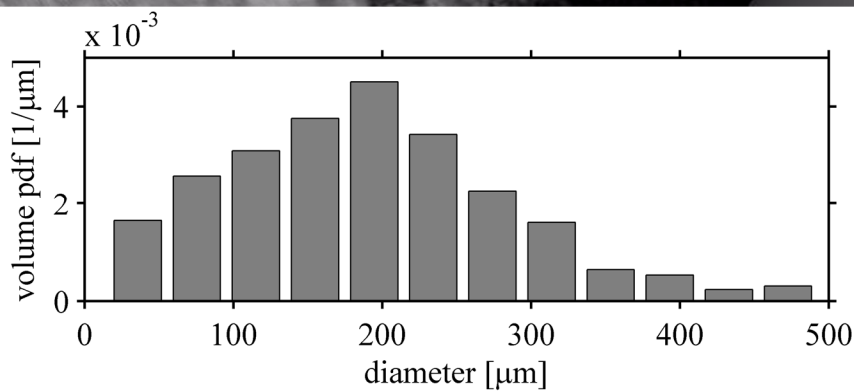
particles ejected from the surface of a burning propellant
captured with 3D holography, $t = 0.00$ ms



Recorded at
20,000 fps
Camera: Photron SA-
Z
Laser: Coherent
Verdi V6

43,684 frames →
▪ 15,991 drops
▪ mass flux =
0.24 mg/s·mm²

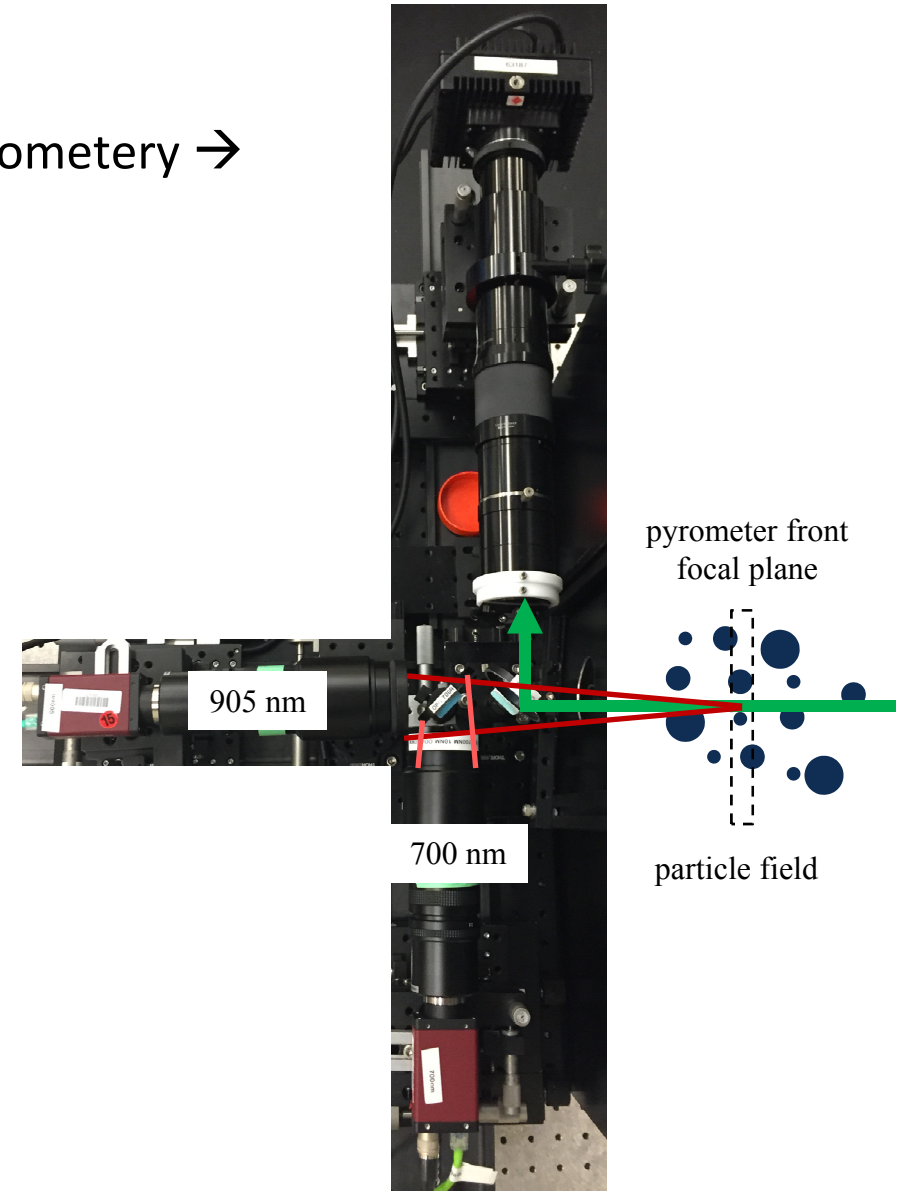
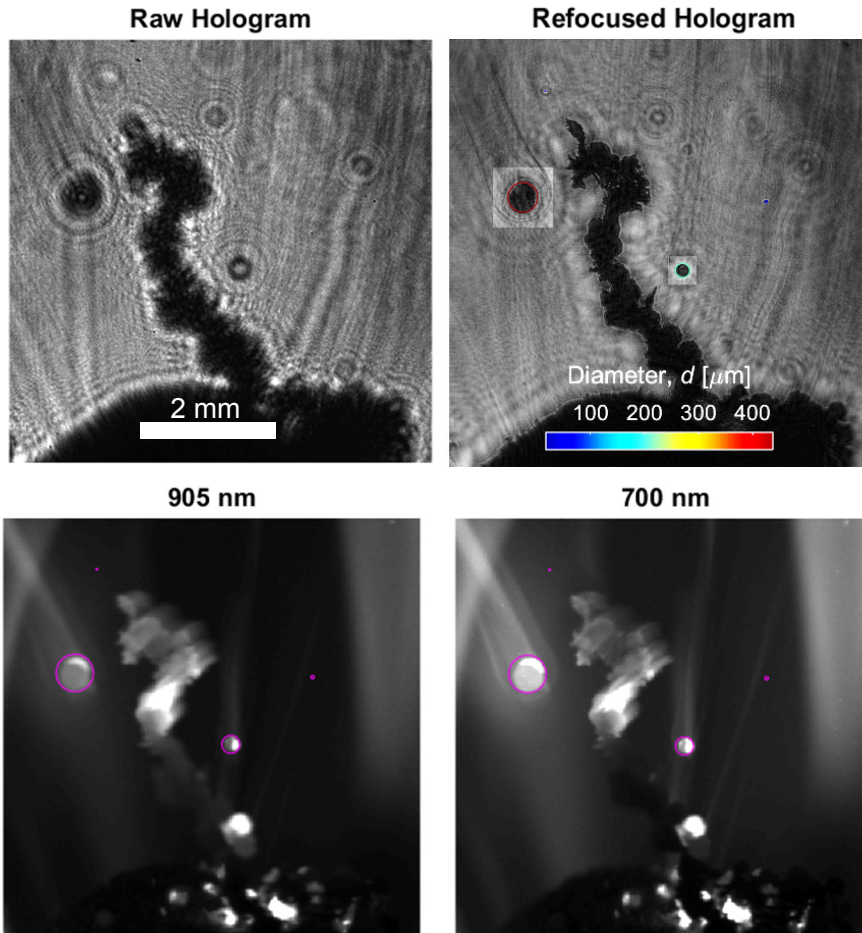
From burn rate and
known composition,
expected mass flux is



Particle temperature measurements

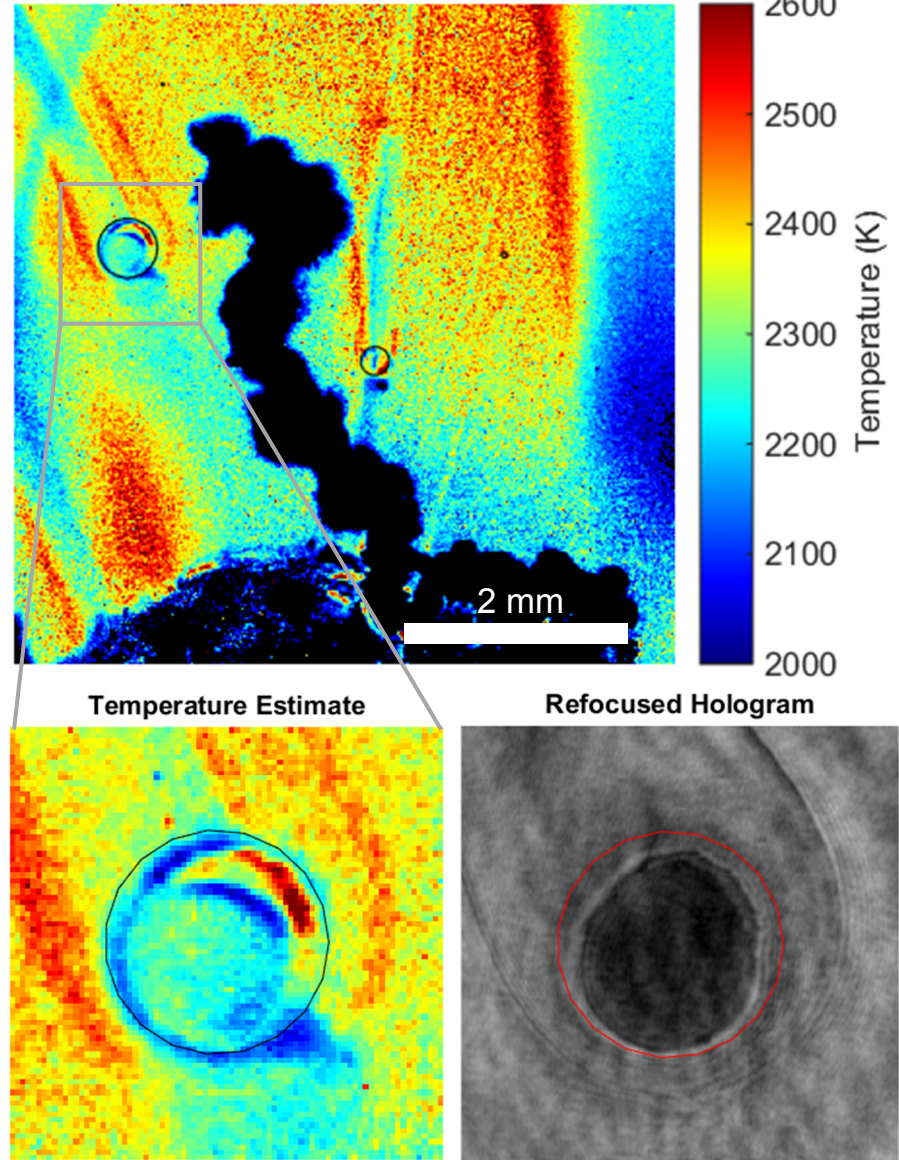
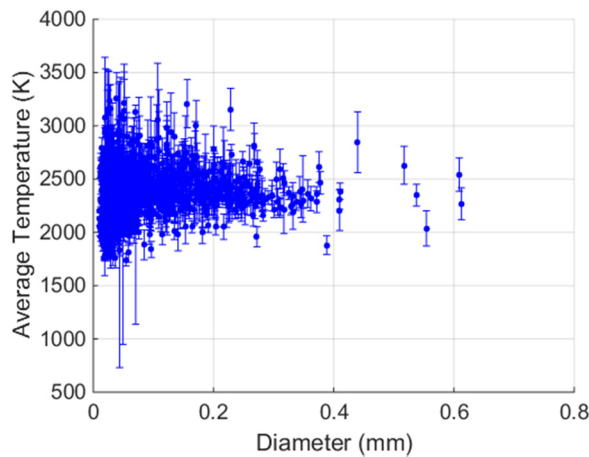
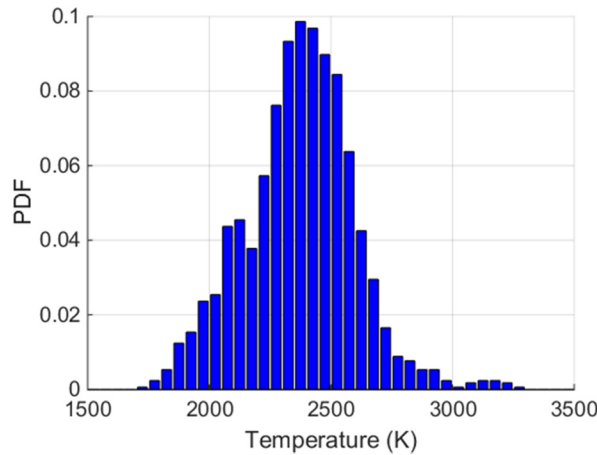
We also need to quantify heat transfer

- Combination of DIH and two-color pyrometry →
particle size + velocity + *temperature*



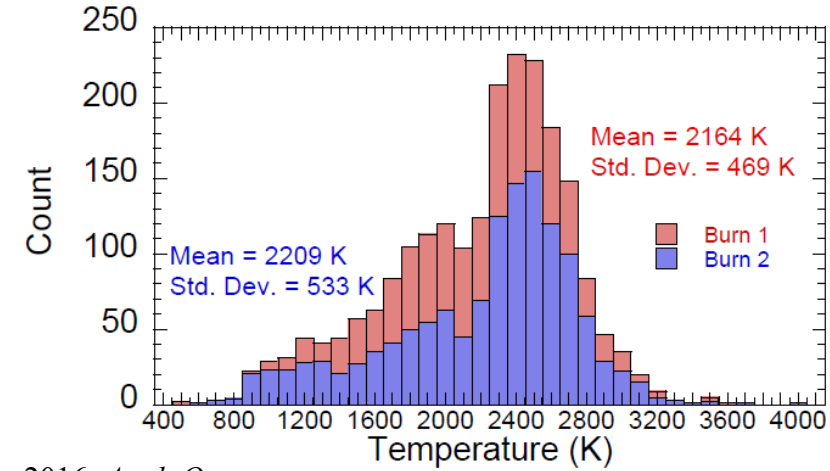
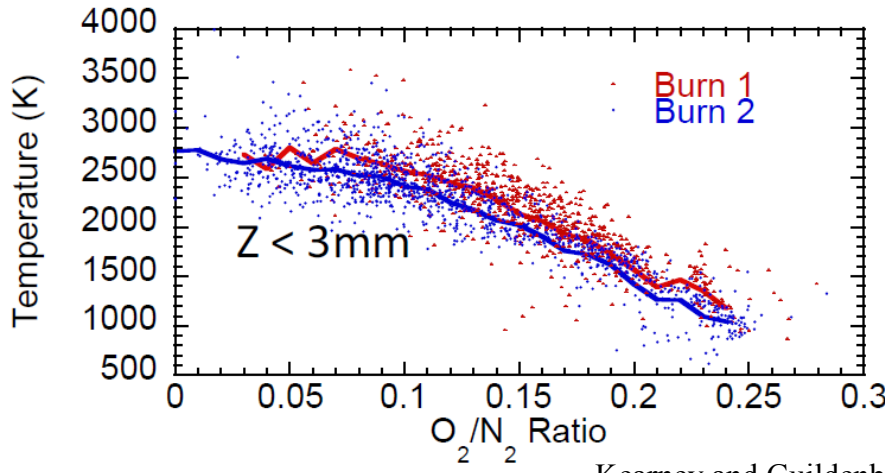
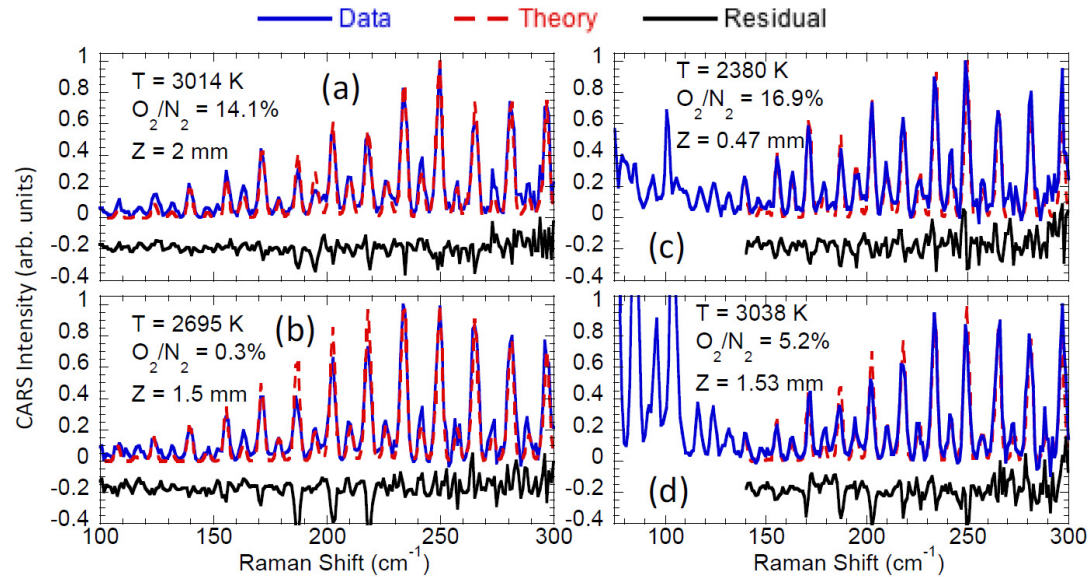
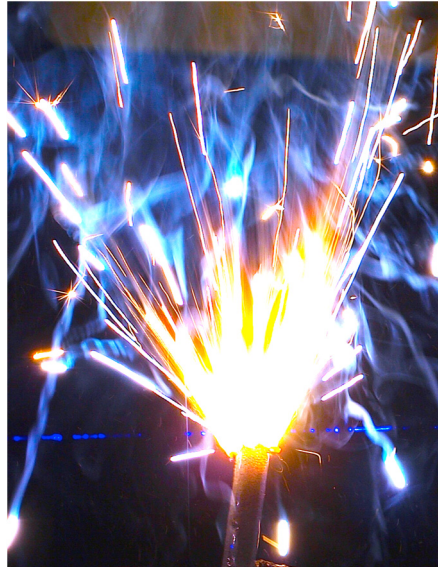
Particle temperature measurements

Assuming graybody emission,
calibrated ratio imaging gives an
estimate of particle temperatures



Gas-phase temperatures with CARS

S. Kearney is measuring gas-phase temperatures using fs/ps CARS

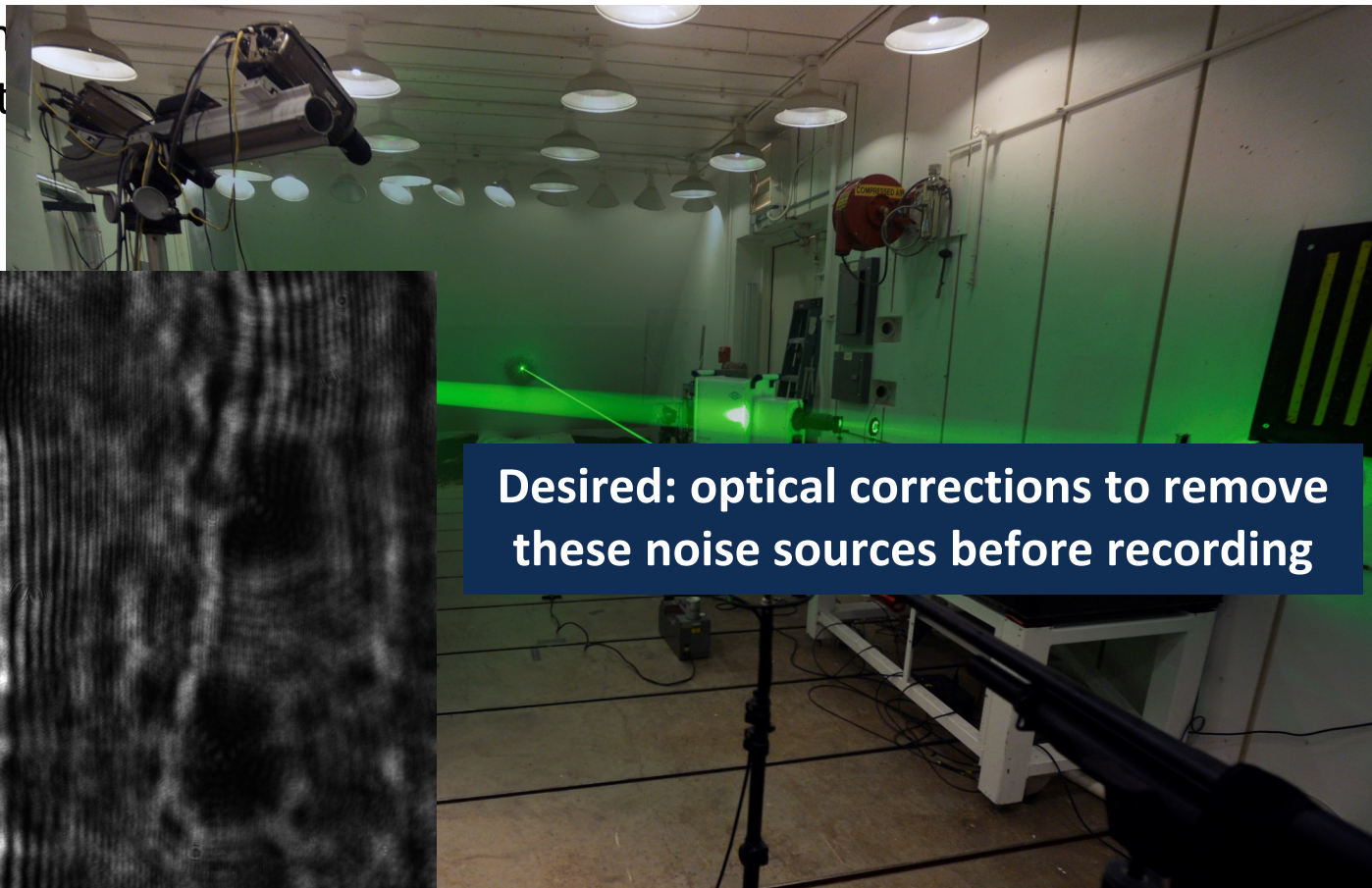


Kearney and Guildenbecher, 2016, *Appl. Opt.*

Optical challenges in DIH

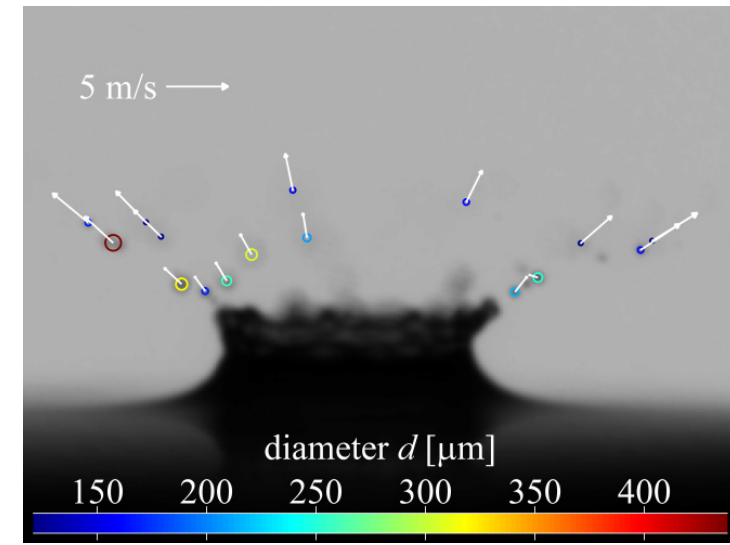
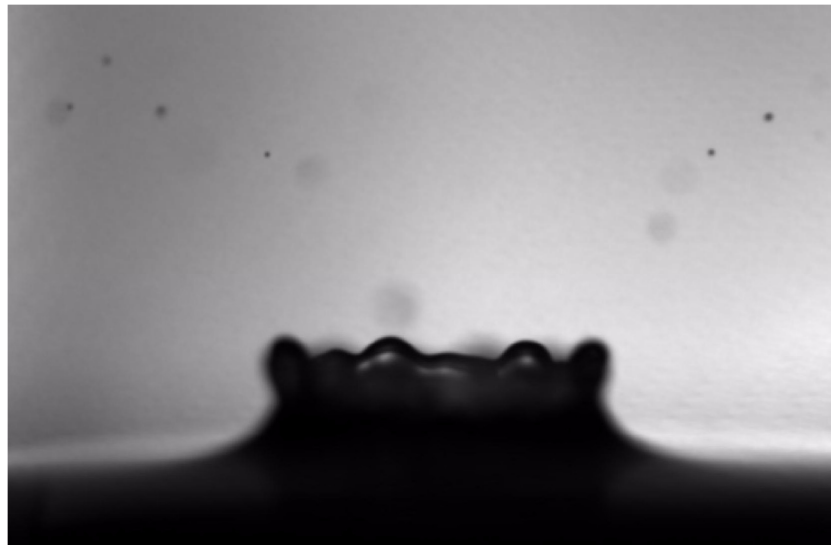
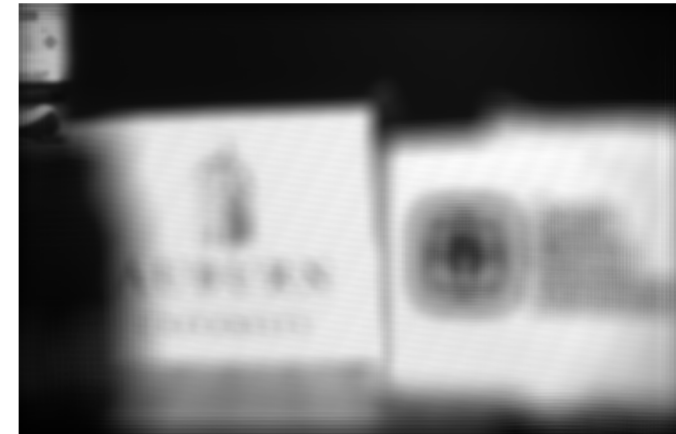
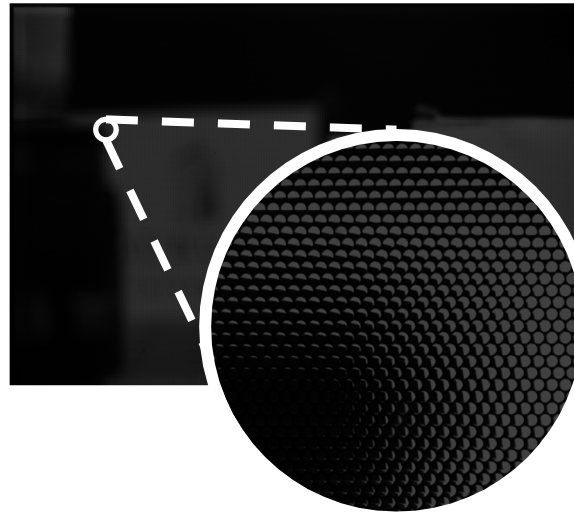
Coherent imaging is susceptible to:

- Image distortion through index of refraction gradients
- Loss of phase information due to multiple-scattering



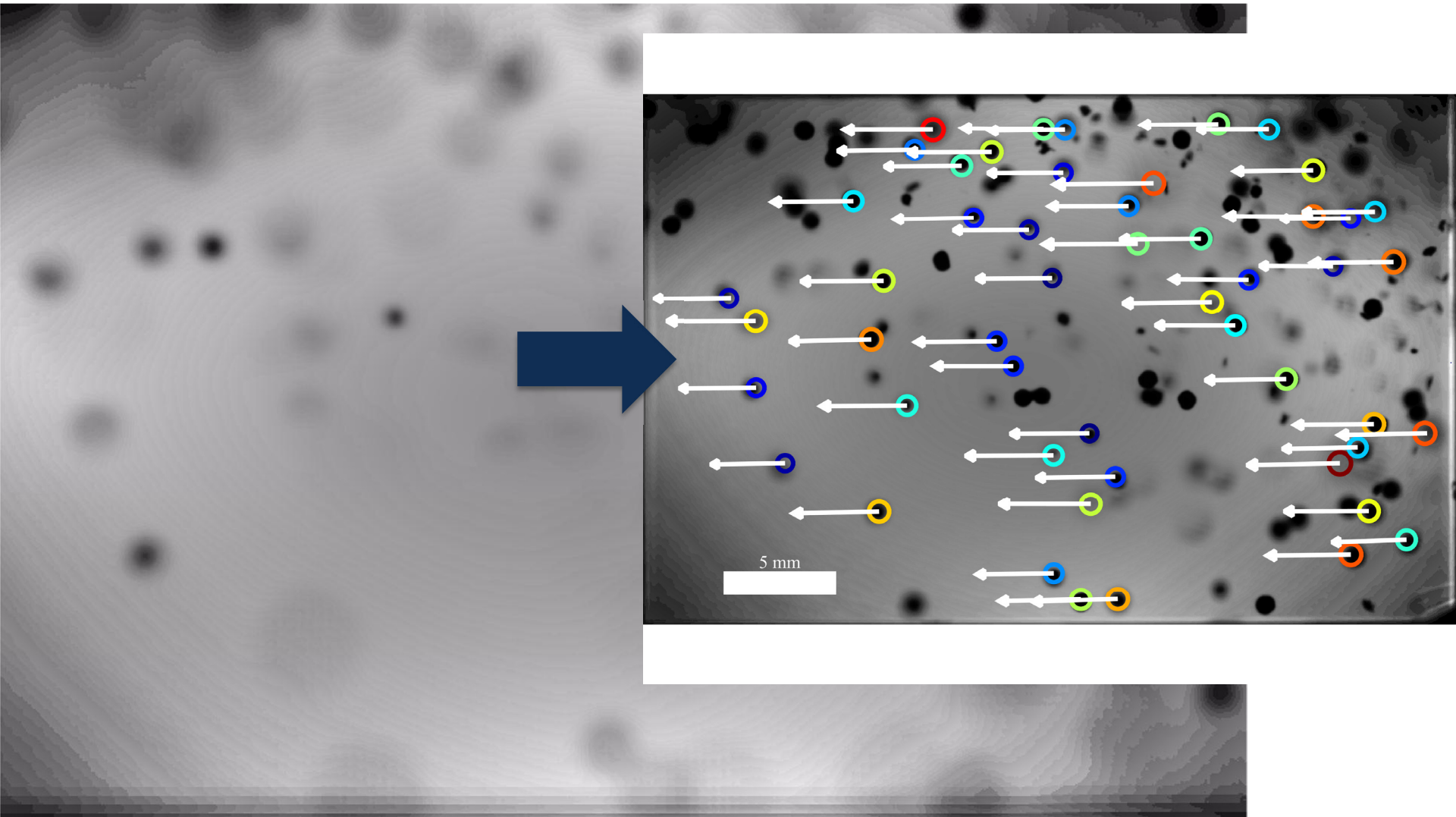
Alternative 3D measurements

Plenoptic cameras use micro-lens arrays and white light to create a 3D image



Alternative 3D measurements

Plenoptic imaging of a shotgun



Conclusions

DIH has many advantages:

- 3D-3C measurement
- Rapid quantification of statistics
- Simple optical configuration

... and opportunities for research:

- Depth-of-focus problem
- Data processing
- Optical improvements

Acknowledgements:

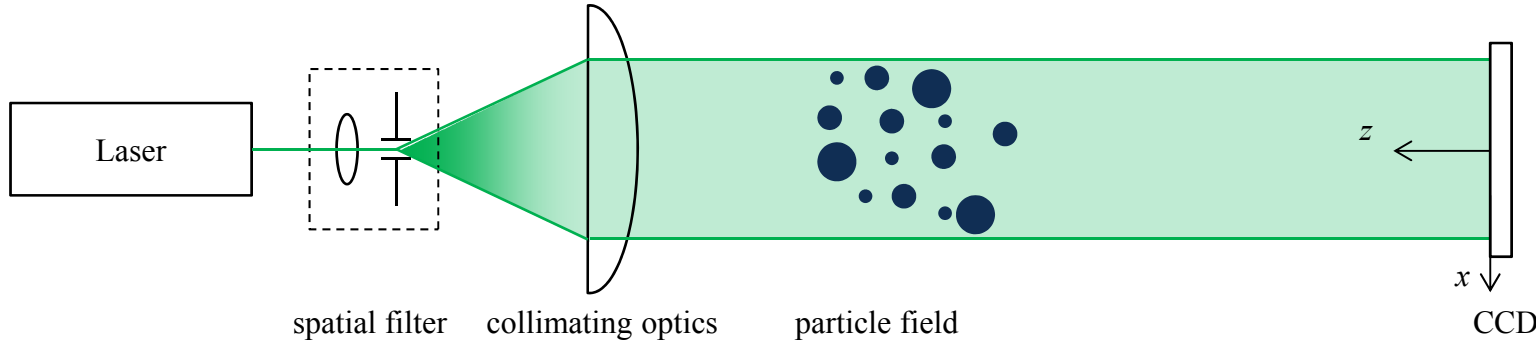
This work was supported by the Laboratory Directed Research and Development and the Weapons Systems Engineering Assessment Technology program at Sandia National Laboratories (SNL)

Many thanks to all of my excellent collaborators: *Jian Gao* (Johns Hopkins University), *Phillip L. Reu* (SNL), *Jun Chen* (Purdue University), *Sean P. Kearney* (SNL), *Kathryn G. Hoffmeister* (SNL), *Paul E. Sojka* (Purdue University), *Thomas W. Grasser* (SNL), *H. Lee Stauffacher* (SNL), *Marcia A. Cooper* (SNL), *Luke Engvall* (University of Colorado), *Justin L. Wager* (SNL), *Thomas A. Reichardt* (SNL), *Paul A. Farias* (SNL), *Joseph D. Olles* (SNL), *Ellen Y. Chen* (SNL), *Brian S. Thurow* (Auburn University), *Elise D. Munz* (Auburn University), *Timothy J. Miller* (SNL), and many others....

Questions

Backup slides

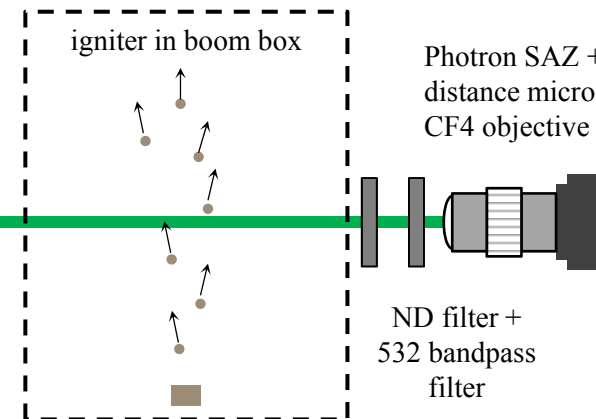
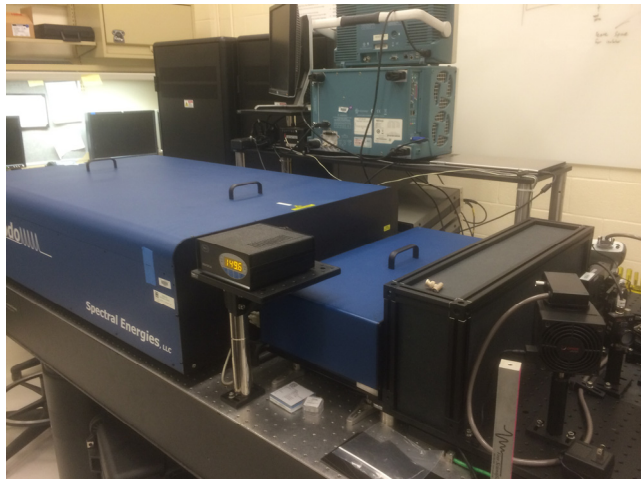
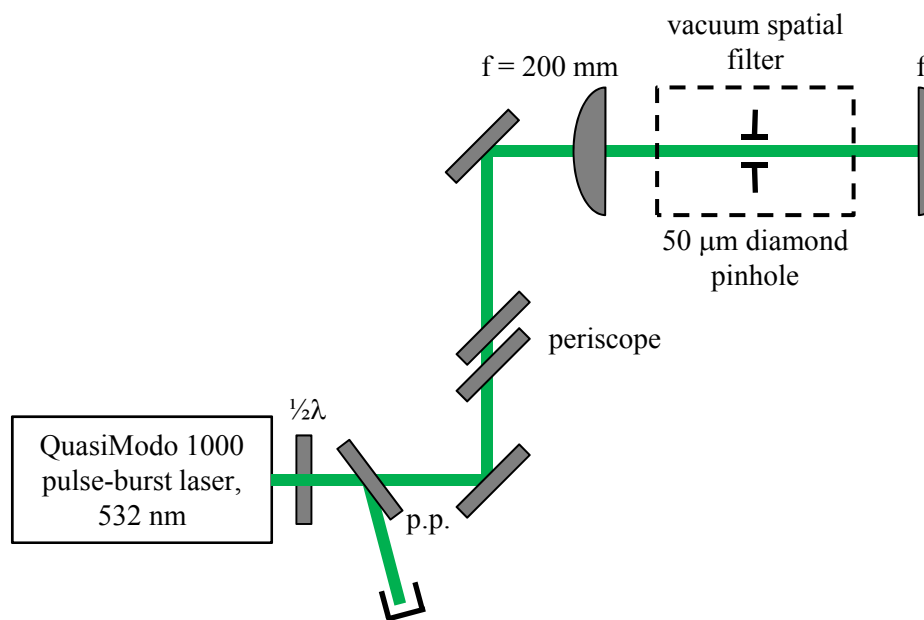
Where is the reference wave?



Hologram is the combination of object and reference waves: $h = |E_o + E_r|^2$

- Reconstruction with E_r gives: $h \cdot E_r = \underbrace{(|E_o|^2 + |E_r|^2)E_r}_{\text{DC term}} + \underbrace{|E_r|^2 E_o}_{\text{virtual image}} + \underbrace{E_r^2 E_o^*}_{\text{real image}}$
 - In off-axis holography, these terms are spatially separated as we attempt to reconstruct the original object wave, E_o
- In in-line holography, we actually want to reconstruct the combination of the reference wave and object wave, $E_o + E_r$
 - Rearranging: $h \cdot E_r = \underbrace{|E_o|^2 E_r}_{\text{DC term}} + \underbrace{|E_r|^2 (E_o + E_r)}_{\text{virtual image}} + \underbrace{E_r^2 E_o^*}_{\text{real image}}$

Pulse-burst DIH



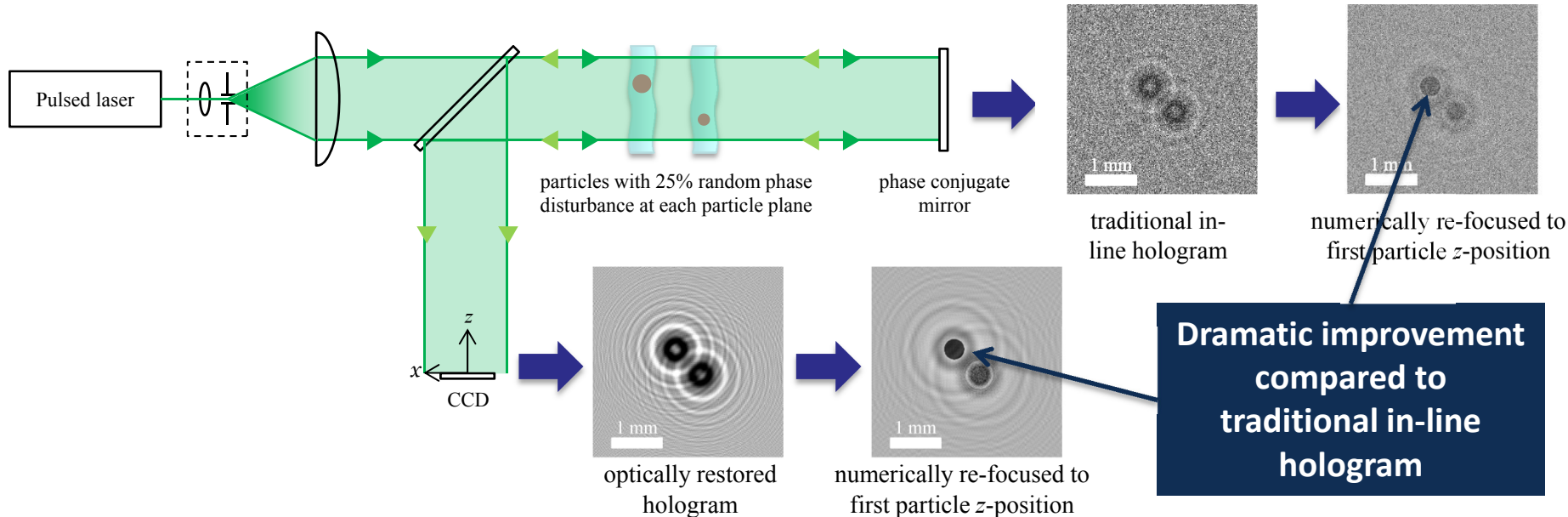
Pulse-burst DIH

$t = 0.00 \text{ ms}$

1 mm

- Beam quality is sufficient for DIH
- Freezes high-speed particles and penetrates through flash and smoke
- Noise due to soot and index-of-refraction gradients

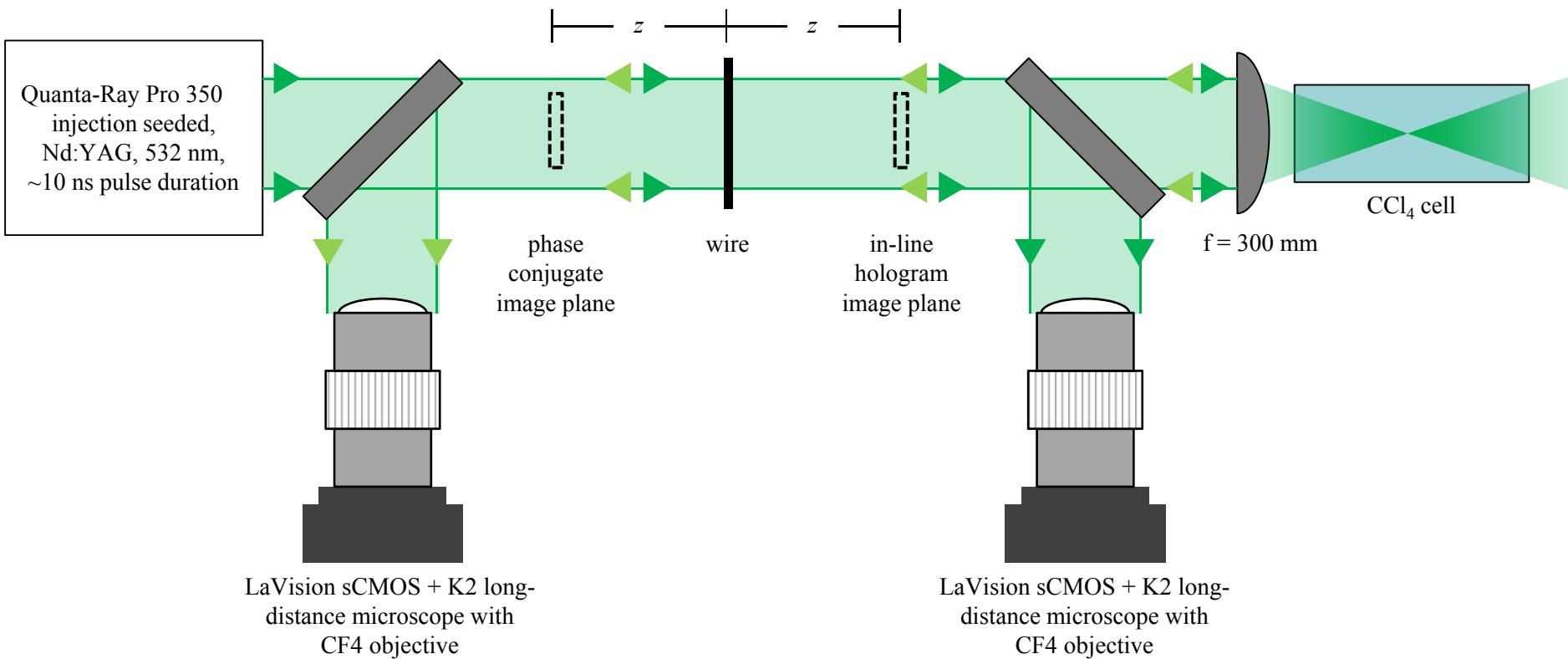
Phase-conjugate DIH theory



- Phase-conjugate mirror reflects the incoming wave with opposite phase
 - Non-linear optical effect achieved through passive means (stimulated Brillouin scattering) or active means (degenerate four-wave mixing)
- After double passing, the phase disturbance is canceled

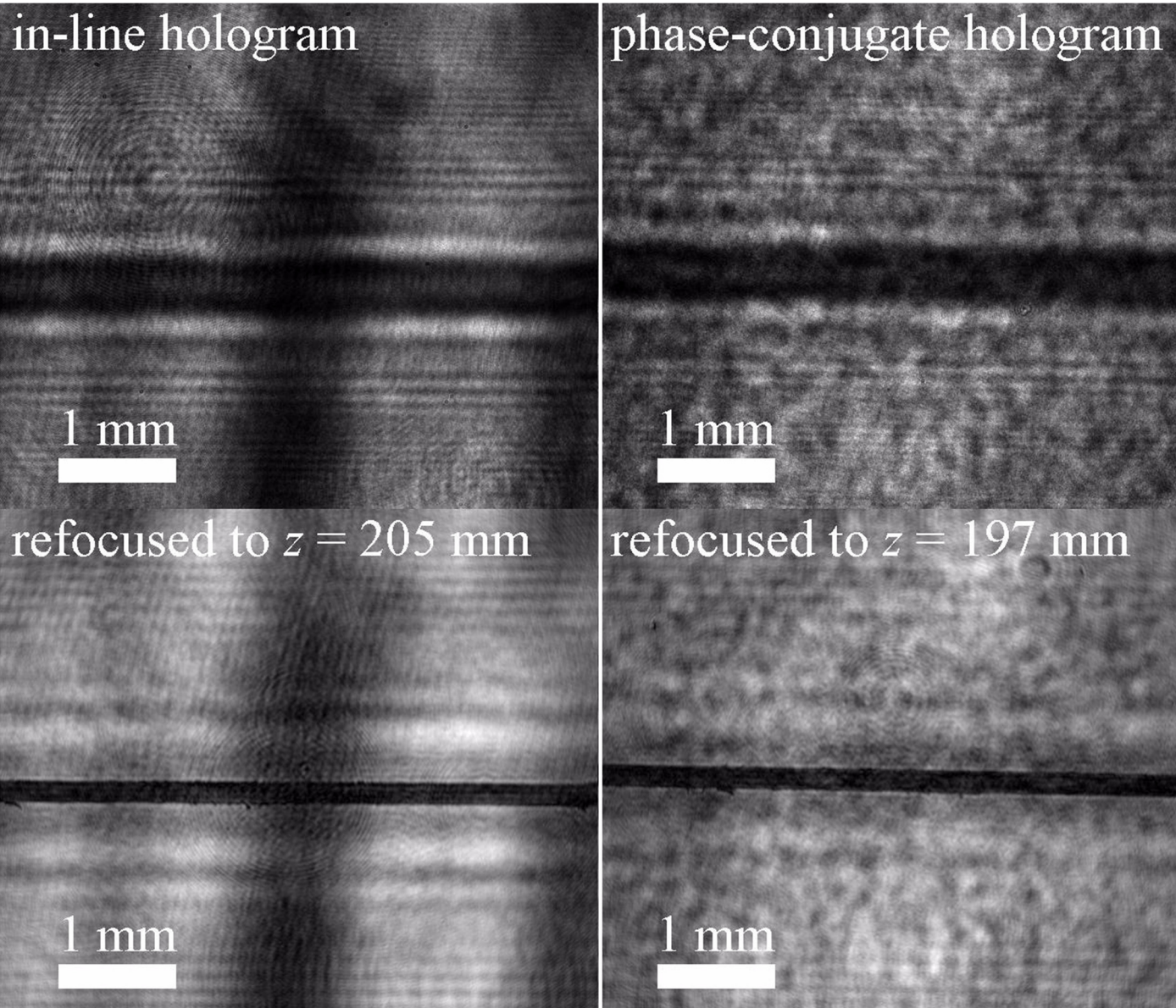
SBS phase-conjugate DIH

A focused beam in a non-linear medium induces phase conjugation via stimulated Brillouin scattering (SBS)



SBS phase-conjugate DIH

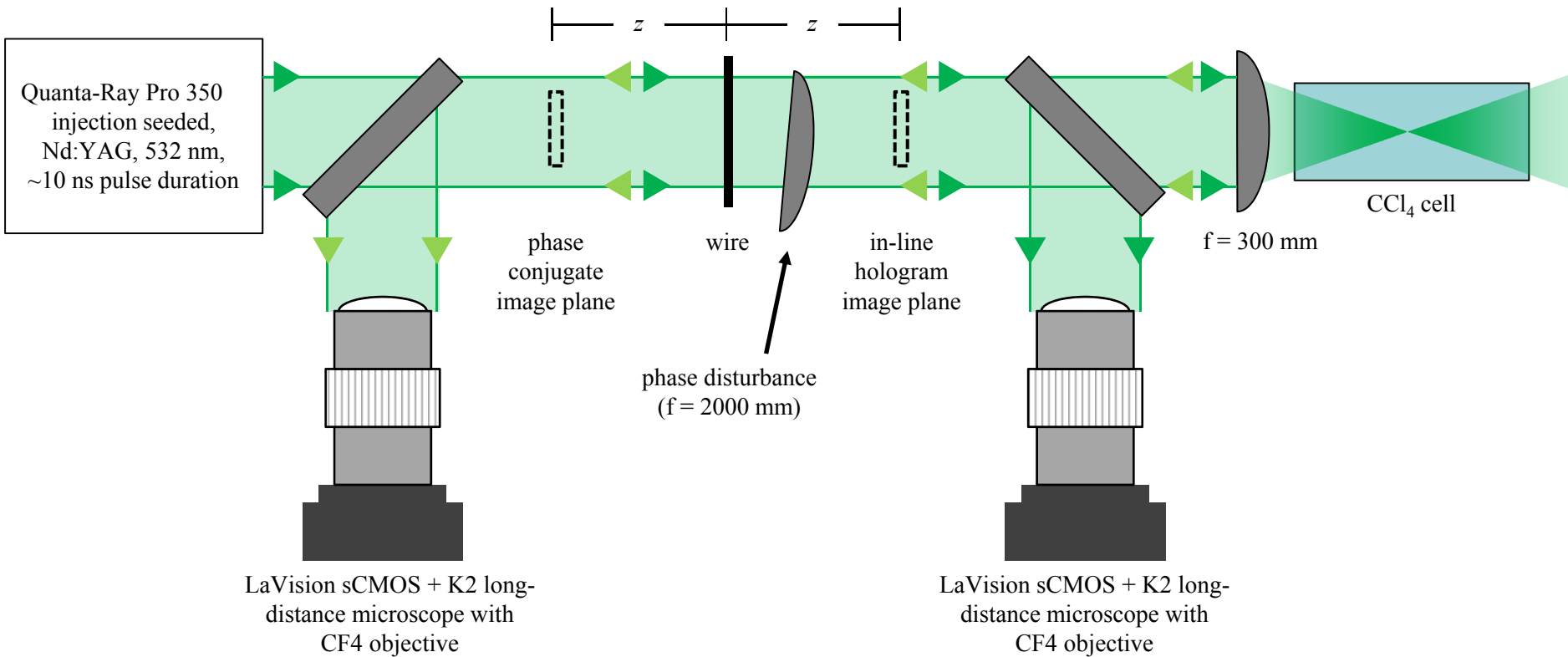
Without a
disturbance
both views give
similar results



SBS phase-conjugate DIH

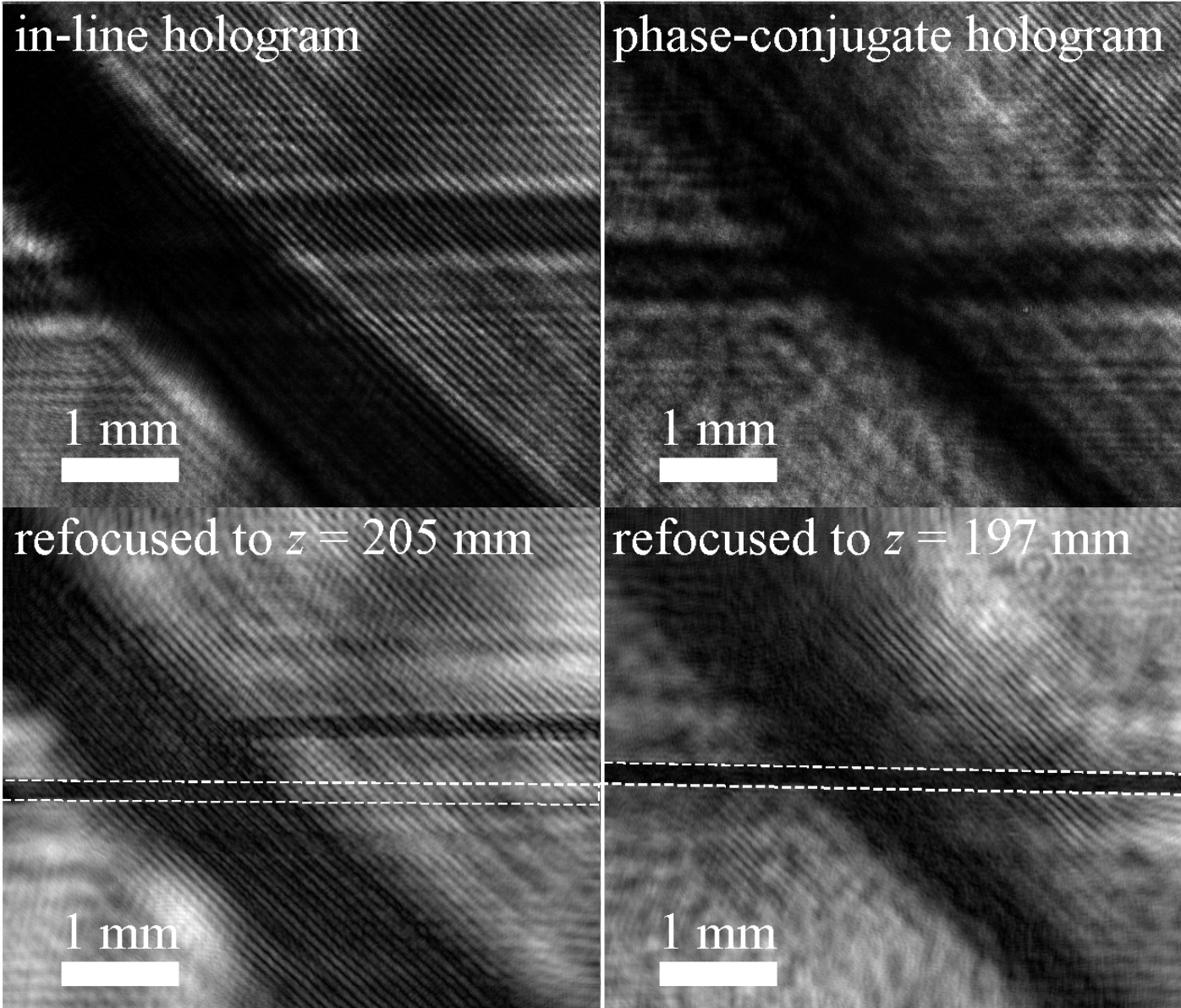
A focused beam in a non-linear medium induces phase conjugation via stimulated Brillouin scattering (SBS)

- A misaligned lens in the beam path causes a phase disturbance



SBS phase-conjugate DIH

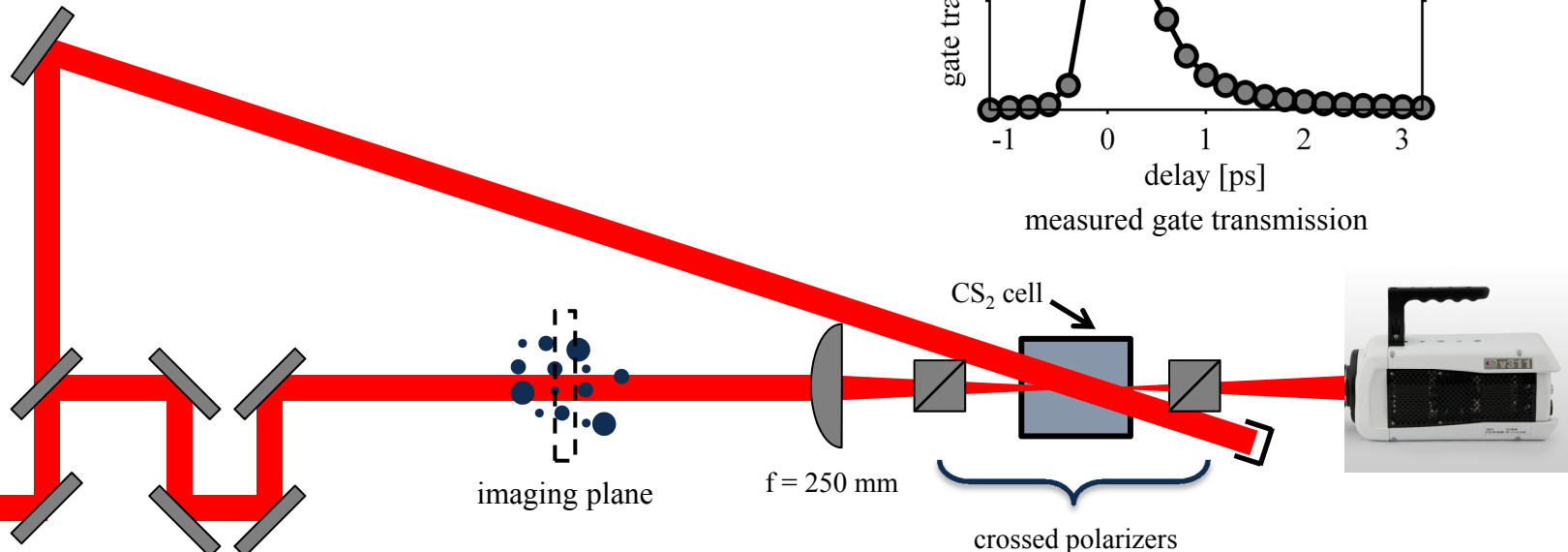
Phase
conjugation
corrects image
distortion



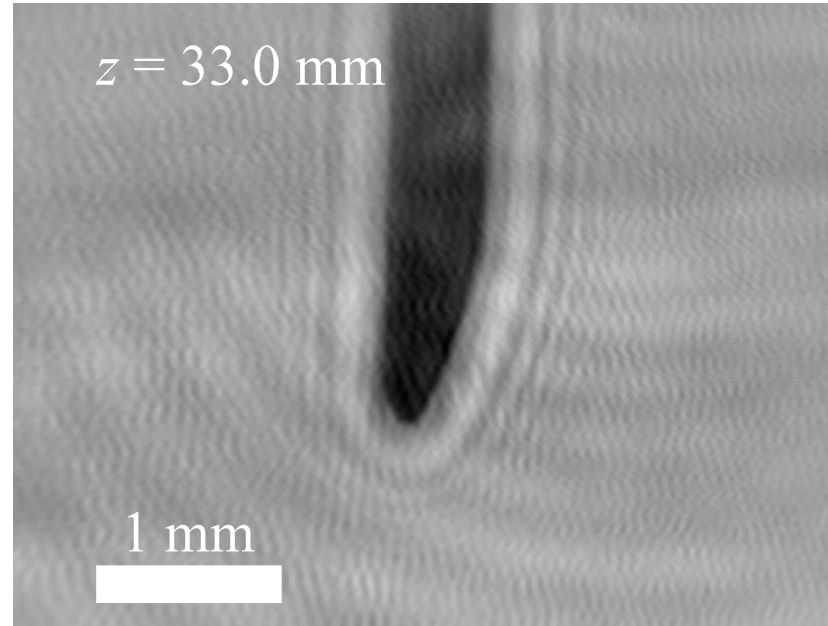
Ballistic DIH

Multiple scattering can be reduced through ps time gating

- Combination with DIH might enable scatter free 3D imaging through optically dense media
 - First proposed by: Trolinger et al 2011, *International Journal of Spray and Combustion Dynamics*



DIH imaging through a Kerr gate (no scatter sources)



DIH image of a needle recorded with the ballistic configuration (1.6 ps switch delay)

Next step: Explore ballistic DIH through dense scattering sources

- Challenge: *Can we retain sufficient image fidelity and coherence to resolve 3D phenomena?*